CHEMISTRY
A European Journal

A Journal of
ChemPubSoc Europe

Accepted Article

Title: Infrared multiphoton dissociation spectroscopy with free electron lasers: On the road from small molecules to biomolecules

Authors: Lucie Jasikova and Jana Roithová

To be cited as: *Chem. Eur. J.* 10.1002/chem.201705692

Link to VoR: http://dx.doi.org/10.1002/chem.201705692

Supported by
ACES

WILEY-VCH

10.1002/chem.201705692

WILEY-VCH

Dedication ((optional))

Infrared multiphoton dissociation spectroscopy with free electron lasers: On the road from small molecules to biomolecules

Lucie Jašíková[a] Jana Roithová(s)*[a]

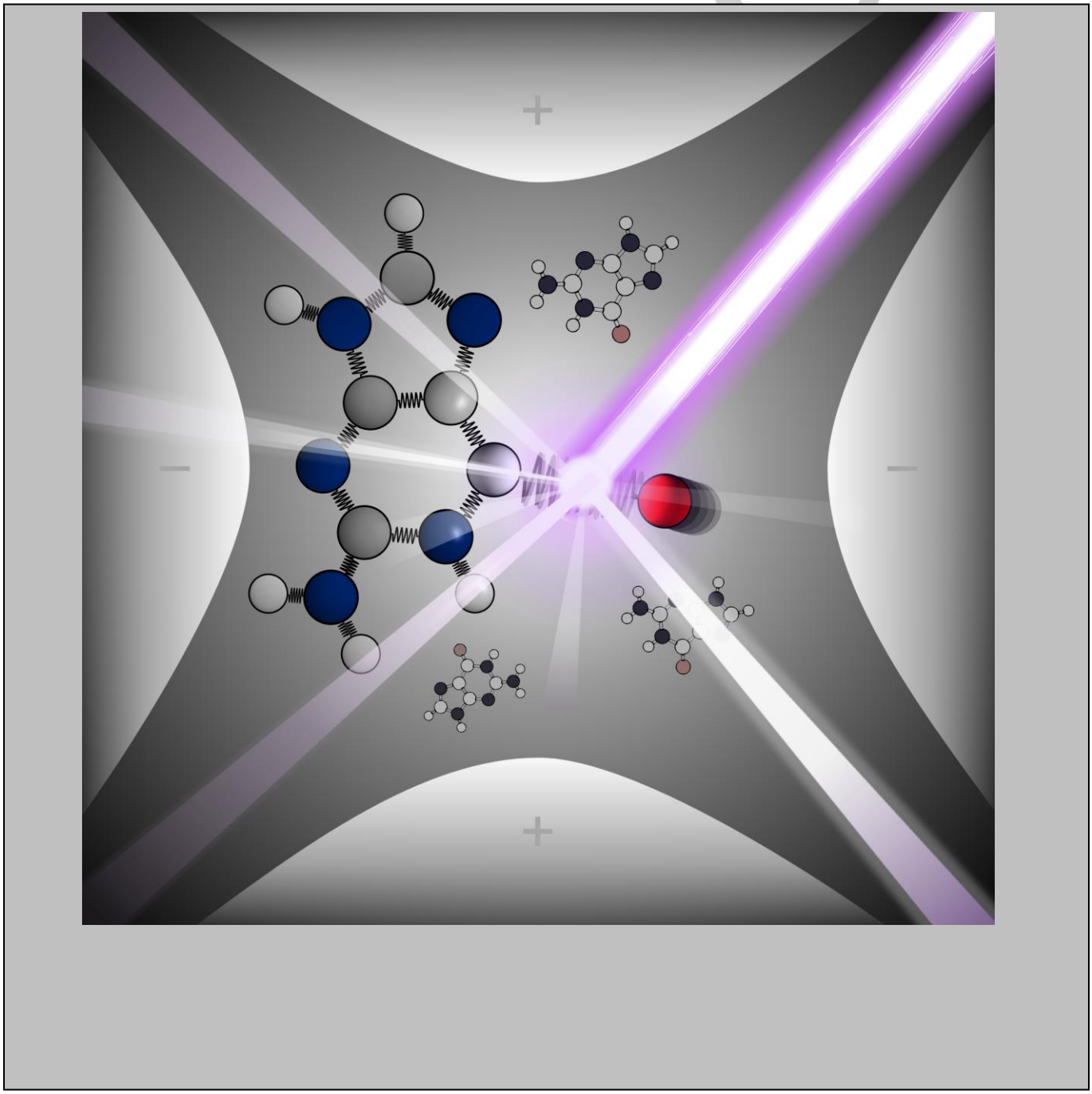

Abstract: Infrared multiphoton dissociation (IRMPD) spectroscopy is commonly used to determine the structure of isolated, mass-selected ions in the gas phase. This method has been widely used since it became available at multi-user free-electron laser (FEL) facilities. Thus, in this minireview, we examine the use of IRMPD/FEL spectroscopy for investigating ions derived from small molecules, metal complexes and organometallic compounds and biorelevant ions. Furthermore, we outline new applications of IRMPD spectroscopy to the study of biomolecules.

1. Introduction

Mass spectrometry is a powerful method with increasing applications in biochemistry, biology, medicine, environmental science and many other fields. The growth of mass spectrometry has been enabled by continuous developments in instrumentation, and improved data analysis. Moreover, mass spectrometry has been coupled with other orthogonal methods. Therefore, this review focuses on the coupling of mass spectrometry with optical spectroscopy of mass-selected ions, particularly infrared multiphoton dissociation (IRMPD) spectroscopy using free electron lasers.

Infrared photodissociation spectroscopy was introduced in the 1980s. Initially, this method was limited to a few laboratories with specialised instrumentation.[1,2] In the beginning of 21st century, IRMPD spectroscopy became available at free electron laser facilities.[3] Free electron lasers operate as facilities and are, therefore, available to many researchers. This availability has considerably broadened the scope of the method. Therefore, IRMPD spectroscopy became a new standard method and significantly increased possibilities of mass spectrometry. Here, we will focus on research using IRMPD spectroscopy with free electron lasers, describing the development of IRMPD spectroscopy from a novel tool to a standard technique and outlining future perspectives.

1.1. IRPMD spectroscopy

Photodissociation spectroscopy provides optical spectra of mass-selected ions in the gas phase. Optical absorption by mass-selected ions cannot be recorded by photon detection because mass spectrometers operate with only a small number of ions (10^3 - 10^6). Consequently, the low number of absorption events is insufficient to significantly alter photon transmission. Therefore, photodissociation spectroscopy takes advantage of a different process. The isolated ions in the gas phase cannot easily dissipate their internal energy. Thus, photon absorption leads to an increase in the internal energy of the ions. If the internal energy rises above the dissociation limit, the ions dissociate. Thus, photon absorption can be detected by ion fragmentation - this phenomenon is detected with ultra-high efficiency by mass spectrometry.

The best, single-molecule method to determine ion structure is infrared (IR) spectroscopy because IR spectra reflect bond vibrations. The energies of IR photons range from less than 0.1 to 0.5 eV (from the 10^2 cm^{-1} range to 4000 cm^{-1}). This energy suffices to dissociate weakly bound complexes or ions with low-energy dissociation pathways. This precondition and the limited availability of tunable IR photon sources limited the subjects initially studied. The first infrared photodissociation spectra were obtained for simple few-atomic ions, such as hydrogen clusters H_5^+ or H_7^+ or protonated hydrocarbons.[2] Several laboratories continued developing this technique and used it to investigate many carbocation complexes with weakly bound tags, such as rare atoms or metal complexes with weakly bound ligands.[4,5]

The boom of research topics addressed by IR photodissociation spectroscopy followed the implementation of infrared free electron lasers.[3] These powerful photon sources operate in the fingerprint range of IR spectra (~600 – 2000 cm^{-1}) with a high flux. The high flux supports repetitive absorption of IR photons. Therefore, isolated ions can accumulate sufficient energy to break covalent bonds. Thus, free electron lasers enabled obtaining fingerprint IR spectra of essentially any ion. We will describe applications in the fields of small molecules, metal complexes, organometallic compounds and bio-relevant ions.

[a] Dr. Lucie Jašíková, Prof. Dr. Jana Roithová
Department of Organic ‘Chemistry
Faculty of Science, Charles University
Hlavova 2030, Prague 2, 128 43, Czech Republic
E-mail: roithova@natur.cuni.cz

Lucie Jašíková studied organic chemistry at Charles University in Prague, Czech Republic (PhD, 2016). Her doctoral research focused on gold-catalysed reactions. Now she works as research fellow together with Professor Jana Roithová at Charles University. She is developing techniques to study reaction intermediates by mass spectrometry and ion spectroscopy.

Jana Roithová obtained her PhD in 2003 (University of Chemistry and Technology Prague). After her postdoctoral research at the Technical University Berlin, she started her research group at Charles University, in Prague, in 2007 and became a full professor in 2014. Her research group focuses on studying reaction mechanisms and developing new methods in mass spectrometry.

2. Small molecules

Most reported IRMPD spectroscopy research was performed with rather “small” ions because larger ions have more complex IR spectra. The spectra of these larger ions are more difficult to interpret and, therefore, it is more difficult to distinguish isomeric ions. The interpretation of IRMPD spectra is usually based on comparisons with theoretical predictions of IR spectra of all feasible isomers of the ions. The theoretical

calculations are usually based on density functional theory.[6] Current hardware capacities allow us to compute molecules with up to a hundred heavy atoms. However, these calculations are not standardly used for molecules above this threshold. In this section we will showcase two studies that highlight the power of IRMPD spectroscopy for studying and understanding the properties of small molecules.

2.1. Where is the charge?

All ions discussed in this review were produced by electrospray ionisation (ESI). However, electrospray ionisation may affect ion structure and composition when transferring ions from solution to the gas phase. During the ESI process, the concentration of molecules and ions in the solution increases, molecules are charged and ultimately desolvated. These processes may lead to protonation or to the association of neutral molecules with metals in solution (sodiated molecules are typically generated by ESI). Furthermore, molecules that are protonated or charged in solution may become different isomers in the gas phase due to sequential reactions during the electrospray process. Accordingly, IRMPD spectroscopy was used to study these processes.[7] In this section, we review how ESI affects the anions formed by *p*-hydroxybenzoic acid deprotonation towards assessing whether these anions have the structure typical for solution or typical for the gas phase.[8]

Deprotonation of *p*-hydroxybenzoic acid can lead either to carboxylate anions (C^- in Scheme 1) or to phenolate anions (P^-). P^- anions are more stable in the gas phase due to stabilisation by electron delocalisation to the aromatic ring. C^- anions are more stable in solution due to the stabilisation by interaction with solvent molecules.

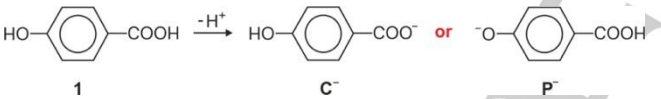

Scheme 1. Single deprotonation of *p*-hydroxybenzoic acid to afford either carboxylate anions (C^-) or phenolate anions (P^-). Reprinted with permission from ref. 8. Copyright 2012 American Chemical Society.

In 2008, Tian and Kass reported that tyrosine deprotonation during the electrospray ionisation process is determined by the solvent, although the structures of the anions are not directly correlated with the C^- type anions in solution.[9] The solvent effect was later clearly shown by Steill and Oomens, who reported IRPMD spectra of *p*-hydroxybenzoic acid deprotonated either at the phenolic or at the carboxylic group.[10] The carboxylate anions have symmetric and anti-symmetric carboxylate stretching bands at 1305 cm^{-1} and 1630 cm^{-1} (highlighted by red bars in Figure 1). The phenolate anions can be traced from the IRPMD spectra by the presence of vibrations associated with the intact COOH group – carbonyl stretch at 1680 cm^{-1} and an in-plane COH bending at 1015 cm^{-1} (blue bars in Figure 1). The results showed that the electrospray ionisation of *p*-hydroxybenzoic acid from protic solvents results in the transfer of the carboxylate anions, i.e., the preferred isomers in solution. Conversely, using aprotic solvents generates phenolate anions, i.e., the energetically preferred isomers in the gas phase.

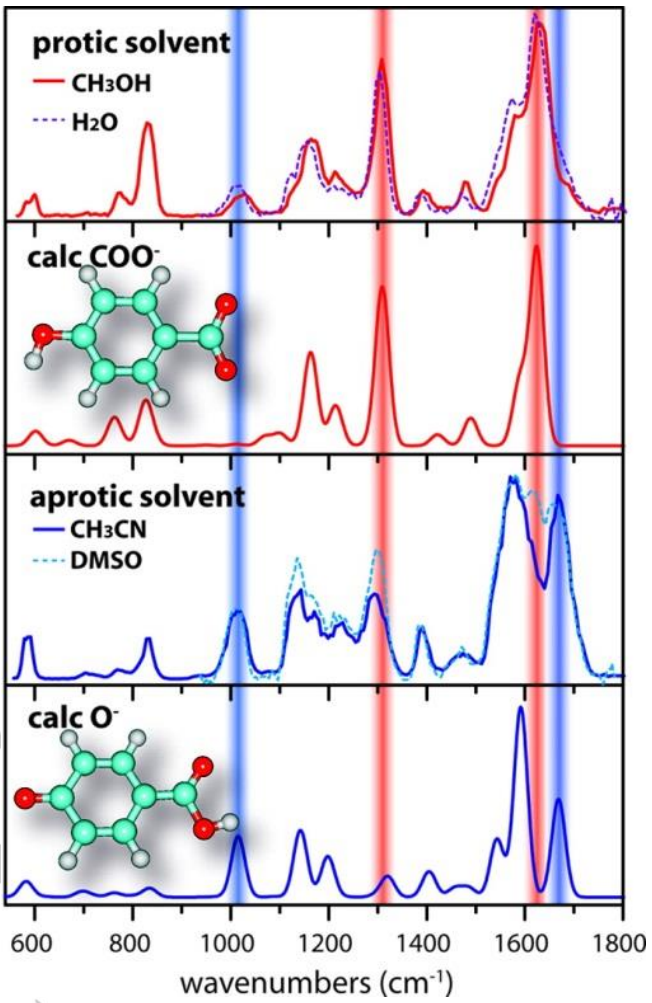

Figure 1. IRMPD spectra of deprotonated *p*-hydroxybenzoic acid generated by ESI from protic (methanol and water) and aprotic (acetonitrile and DMSO) solvents compared to the calculated spectra of carboxylate (C^-) and phenoxide (P^-) isomers. The red and blue bars indicate diagnostic carboxylate and carboxylic acid bands, respectively. Reprinted with permission from ref. 10. Copyright 2009 American Chemical Society.

These results suggested that electrospray ionisation transfers ions from solution to the gas phase without changing the structure. Such a conclusion would indicate that protic solvents favour the deprotonation of the carboxyl group, whereas aprotic solvents favour the deprotonation of the phenol group. However, this is only partly valid. NMR spectroscopy showed that both protic and aprotic solvents favour carboxylate anions in solution.[8] What makes the difference is the effect of solvent molecules on anion stabilisation during the electrospray ionisation process. Carboxylate anions are stabilised by the formation of dimers or larger clusters with molecules of water or methanol, which most likely preserves the solution structure of the anions during the desolvation process. Conversely, the stabilisation of anions in aprotic solvents is most likely achieved by dimerization with other molecules of *p*-hydroxybenzoic acid. These dimers preferentially dissociate into phenolate anions in the gas phase.[8] In conclusion, the structure of the ions produced by electrospray ionisation depends on several factors, particularly on the type of solvent.

2.2. What is the effect of charge?

Bond-stretching frequencies in infrared spectra depend on the masses of the atoms involved in the bond and on the strength of the bond between these atoms. Intuitively, we understand that positively charging a molecule, either by protonation or by electron removal, weakens the bonds in the molecular ion. Therefore, the stretching bands of the bonds affected by the positive charging are red shifted. However, how is the molecule affected when negatively charged?

Theoretical calculations predicted that the C(2)-H stretching band in the isopropoxy anions is red shifted by several hundreds of wavenumbers with respect to the position of the usual aliphatic C-H stretching bands.[11] This extreme red shift occurs upon *iso*-propanol deprotonation. The oxygen anion forms a partial double bond with the C(2) carbon atom. Therefore, the carbon atom forms a weaker bond with the hydrogen atom. This change in bond strength causes the extreme red shift of the C-H stretching mode.

These theoretical results were confirmed by the IRMPD spectra of several isopropoxy anions.[12] Oomens et al. showed that the C(2)-H stretching of isopropoxy anions is found at frequencies well below those of aldehyde C-H bonds (Figure 2). The aldehyde C-H bond vibrations are the lowest lying C-H vibrations found in common organic compounds. They confirmed the position of the C(2)-H stretching band in the 2200 – 2400 cm^{-1} range by deuterium labelling experiments, thus suggesting that charging molecules both negatively and positively weakens the affected bonds.

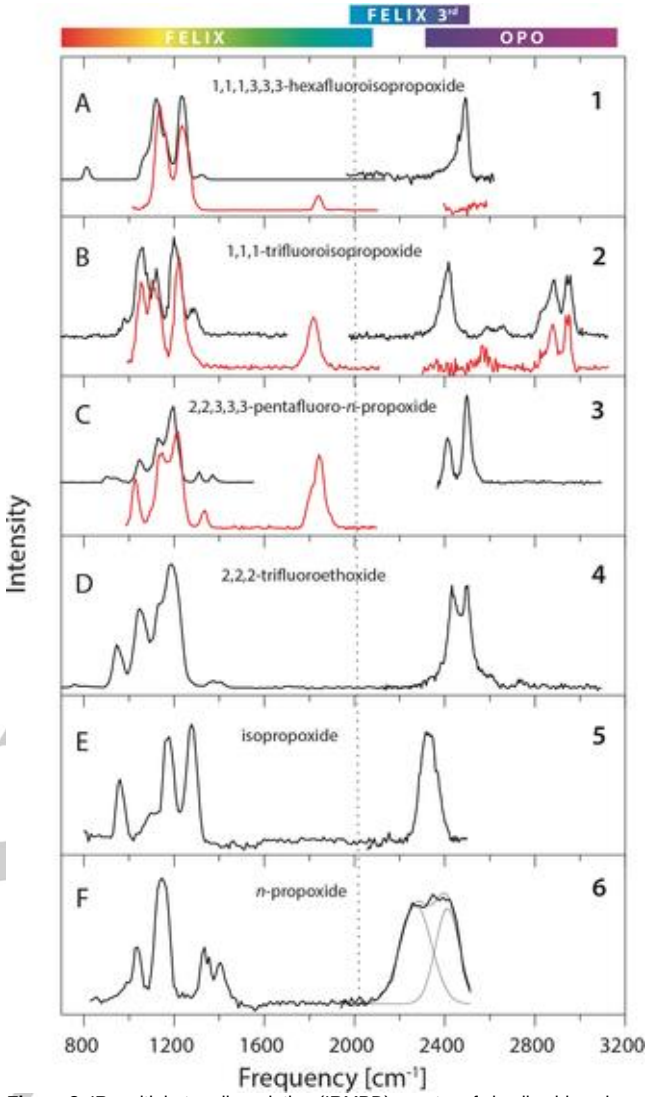

Figure 2. IR multiphoton dissociation (IRMPD) spectra of six alkoxide anions. Traces in red correspond to deuterated analogues, $(CF_3)_2CDO$, $CF_3(CH_3)CDO$, and $CF_3CF_2CD_2O$ anions, respectively. Reprinted with permission from ref. 12 .

3. Bonding interactions

As demonstrated above, IRMPD spectroscopy is a unique tool for assessing bonding patterns and distinguishing isomers. This chapter will show how this tool can be further used to characterise weak interactions. Specifically, we will review how hydrogen-bonding patterns, ion-induced dipole interactions and disperse interactions were investigated.

3.1. Hydrogen bonding

Hydrogen bonding is crucial for the structure of molecules with hydrogen atoms bound to electronegative atoms in non-polar environments or in the gas phase.[13] Several IRMPD spectroscopy studies of protonated, small, biorelevant molecules, such as aminoacids, have already been published.[14] More recently, studies have focused on their proton-bound dimers or larger oligomers.[15] These studies have also addressed the site of protonation of the molecules, the effect of electron-donating groups on the protonation site and on the structural effects of

hydrogen bonding with the neighbouring functional groups. Many of these spectroscopic investigations of hydrogen bonding in mass-selected ionic models were conducted using predissociation spectroscopy or IRMPD spectroscopy with table-top light sources.[16] These methods were chosen because the stretching bands involve hydrogen atoms. These bands usually lie above the frequencies reachable by free electron lasers. Nevertheless, some models were investigated using FELs, and they will be shortly discussed below.

Hydroxonium ions stabilised in the framework of crown ethers can be used as a model for protonated group stabilisation. Hurtado et al. compared the structures of complexes between H_3O^+ and 18c6 ether or 15c5 ether (i.e., [H_3O^+@18c6] or [H_3O^+@15c5]).[17] The H_3O^+ cation and 18c6 ether have C_{3v} symmetry. The cavity of the 18c6 ether has the right size to stabilise the C_{3v} symmetrical binding of the hydroxonium ion (Figure 3). Accordingly, the IRMPD spectrum of [H_3O^+@18c6] is clearly resolved, and it can be well predicted by harmonic IR calculations.

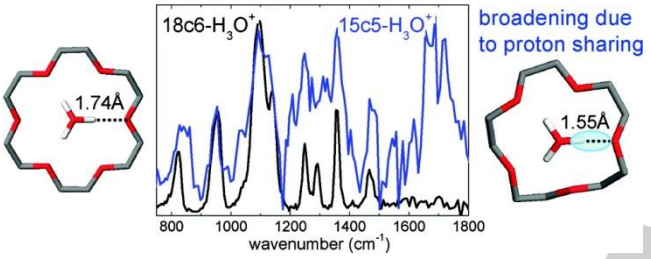

Figure 3. IRMPD spectra of 18c6-H_3O^+ (black) and 15c5-H_3O^+ (blue) complexes. The most stable structures of 18c6-H_3O^+ and 15c5-H_3O^+ complexes calculated at the B3LYP/6-31++G(d,p) level of theory. Reprinted with permission from ref. 17. Copyright 2011 American Chemical Society.

Hydroxonium ion encapsulation into the smaller 15c5 crown ether with lower symmetry leads to a distortion. Hydroxonium forms one shorter and two longer hydrogen bonds with the crown ether. As a result, the IRPMD spectrum of [H_3O^+@15c5] contains an additional band above 1600 cm^{-1} that corresponds to the H-O-H bending mode. Furthermore, the complex can attain several similar close-energy conformations, which lead to the overall broadness of the bands in the IRMPD spectrum.

A closer look at the symmetrical [H_3O^+@18c6] complex shows that the H_3O^+ ion is at the central symmetrical position due to the “anti-cooperative effect” of the tridentate ligand. This anti-cooperative effect results from the compensation of the binding energies of the oxygen atoms of the crown ether to the hydroxonium ion, and none of these bonds prevail over the others. This effect prevents proton transfer from H_3O^+ to the crown ether. Such proton transfers occur between H_3O^+ and simple dialkyl ethers because ethers have larger proton affinities than water. Hence, the constrained tridentate environment of 18c6 holds the proton at the hydroxonium ion.

The research groups of Johnson and McCoy recently reported that the [H_3O^+@18c6] complex has very broad vibrational bands in the range of O-H stretches.[18] They found that these broad bands can be explained by strong anharmonic coupling between the O-H stretching vibration and the translational movement of the H_3O^+ ion towards one of the oxygen atoms of the ether. Similar diffuse bands were previously observed in many studies of solvated hydroxonium ions.[19] Hence, the constrained [H_3O^+@18c6] model helped to explain the origin of these diffuse bands.[18,20]

Another model for hydrogen bonding interactions focuses on the binding between ammonium groups and halide anions (X^-). This type of interaction can be important in protein chemistry, particularly when assessing the effect of the halide anion on this hydrogen bonding. The simplest model to investigate would be [$(NH_4)^+$…X^-…$(NH_4)^+$]. However, this complex is not linear, which would be desirable for a systematic study. The ammonium groups interact not only with the halogen anion but also with each other.[21] Demireva et al. circumvented this problem by studying complexes of halides with α,ω-diaminoalkanes.[22] They used deuterated amines to observe the hydrogen bonding using FEL radiation (Figure 4).

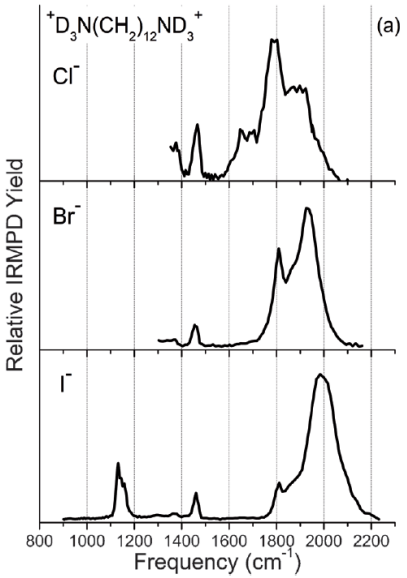

Figure 4. IRMPD spectra at 298 K of deuterated 1,12-dodecanediamonium complexes with Cl^- (top), Br^- (middle), or I^- (bottom) halide anions. Reprinted from ref. 22.

The hydrogen bonding between the ammonium groups and the halogen anion in [$(D_3N^+$-$(CH_2)_{12}$-ND_3^+…X^-] is identified in IRMPD spectra as a broad band in the 1700 – 2100 cm^{-1} range (Figure 4). The bands detected for D_3N^+-$(CH_2)_{12}$-ND_3^+ complexes with different halides redshift with the increase in the gas-phase basicity of the halide (I^- < Br^- < Cl^-). Red-shifting shows increasing hydrogen bonding strength. Note that the hydrogen bonding bands are partly overlapping with bands that originate from the coupling of the N-D stretching frequency with N-D wagging or bending modes. These features could have been de-convoluted based on calculations and analysis.

The authors extended the study by using different carbon chain lengths and by methylation of the amino groups. This approach allowed them to assess the effects of the bonding geometry and gas-phase basicity of the amino groups on the hydrogen bonding (Figure 5). An increase of the basicity of the amino groups weakens the hydrogen bonding (the stretching frequencies blue shift). The weaker hydrogen bonding is less affected by the basicity of the halides (the smaller halide effect

corresponds to a smaller slope of the red line relative to the black line in Figure 5). In turn, the effect of the bonding geometry was tested by using a diamine molecule with a shorter alkane linker. Shortening the linker from twelve to seven CH_2 units changed the almost linear coordination of the ammonium-halide-ammonium unit in the original complex, decreasing the binding angle to 125°. Such a change of binding geometry redshifts the vibrations of the corresponding hydrogen bonds (cf. red and blue points in Figure 5, respectively).

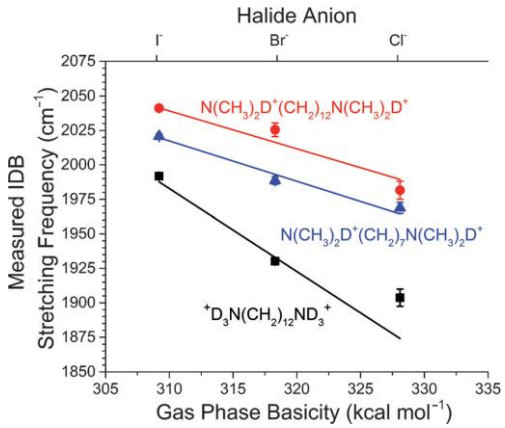

Figure 5. Measured ionic deuterium bond stretching frequency for deuterated 1,12-dodecanediammonium (squares), tetramethyl-1,12-dodecanediammonium (circles), tetramethyl-1,17-heptanediammonium (triangles) as a function of the gas-phase basicity of the halide anion. Error bars indicate the standard error in the ionic deuterium bond stretching frequency. Reprinted from ref. 22.

3.2. Cation-pi interaction

Interaction of π-electrons with cations is best described for aromatic rings (Scheme 2). Aromatic electrophile substitution starts with an attack of a cation to the π-electron system. The initially formed π-complex then rearranges to a sigma complex, which is usually the rate-determining step of the reaction. The groups of Fornarini and Maître have published a series of papers on the IRMPD characterisation of these complexes.[23] Here, we will show an example of the π-complex between benzene and nitrosyl cation, an intermediate in the nitrosation reaction (E = NO in Scheme 2),[24] although it should be noted that several studies on anion-π interactions have also been published.[25]

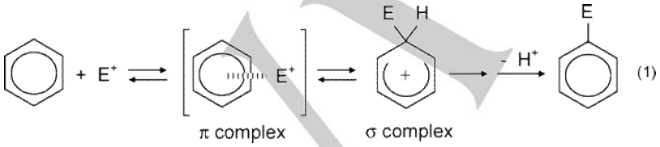

Scheme 2. Aromatic electrophilic substitution. Reprinted with permission from ref.24. Copyright 2006 American Chemical Society.

The positive charge of the nitrosyl cation is located more at the nitrogen atom than at the oxygen atom. Accordingly, the NO^+ cation interacts with the π-electron systems through the nitrogen side. The attractive interactions create a rather shallow potential well with several local minima. The minima can be characterised as η^6 complexes with the NO cation slightly bent off axis (**I**) or as complexes with the NO^+ almost parallel to the ring and with the nitrogen atom pointing towards one of the carbon atoms (**II**).[24]

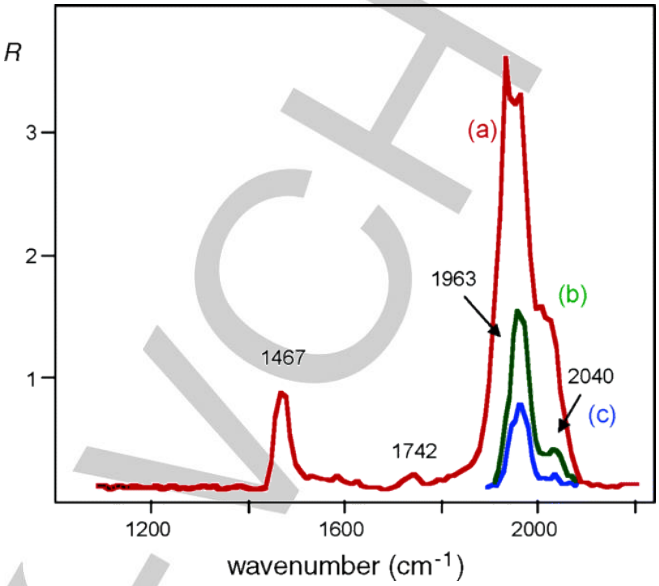

Figure 6. IRMPD spectrum of $[benzene,NO]^+$ ions obtained with full (a) and attenuated (b and c) laser power. Reprinted with permission from ref.24. Copyright 2006 American Chemical Society.

Theoretical calculations predict that both isomers have a strong N-O stretching vibration at approximately 2000 cm^{-1} and weak C-C stretching and ring-deformation vibrations in the range from 1400 to 1600 cm^{-1}. Experimentally, the NO stretching band is found at 1963 cm^{-1} (Figure 6). The band has a side band at approximately 2040 cm^{-1}. This feature results from an anharmonic effect involving C-H vibrations because it disappears in the spectrum of fully deuterated complex ($C_6D_6.NO^+$). Another clear band is located at 1467 cm^{-1}, and it shifts to 1313 cm^{-1} in the spectrum of the deuterated complex. This vibration was attributed to the ring deformation vibrations involving the C-H bonds. The theoretical spectrum of the complex **II** contains more bands in the range of the ring deformation vibrations (4 separate bands are predicted) because it is far less symmetrical than complex **I**. Hence, the experimental spectrum is more consistent with the detection of complex **I** with the η^6 coordinated NO cation.

Another paradigmatic example of addressing cation-π interactions by IRMPD spectroscopy is the study of the interaction between the ammonium group and the aromatic ring.[26] Chiavarino et al. chose a C_6H_5-$(CH_2)_n$-NH_3^+ model that allows adjusting the distance of the ammonium group to the aromatic ring by changing the number of the methylene groups in the linker. The distance between the interacting groups is correlated with the strength of the bond between them. Figure 7 shows the spectral range of the N-H vibrations in the most flexible system studied, with n = 4. This ion clearly has two free N-H vibrations above 3300 cm^{-1} and one broad band below 3100 cm^{-1}. The broad band corresponds to the N-H vibration of the bond that is pointed towards the aromatic ring. The 200-cm^{-1} redshift indicates a strong interaction. The broadness of the peak suggests that this ion has several local conformational

minima. The fluctuation between these minima causes small changes in the N-H…π interaction, thereby broadening the peak. Although these results were obtained with a laboratory optical parametric oscillator (OPO) source of photons, this system was also studied in the fingerprint region using FEL. However, the fingerprint spectra were less informative about the hydrogen-bonding effect.[26]

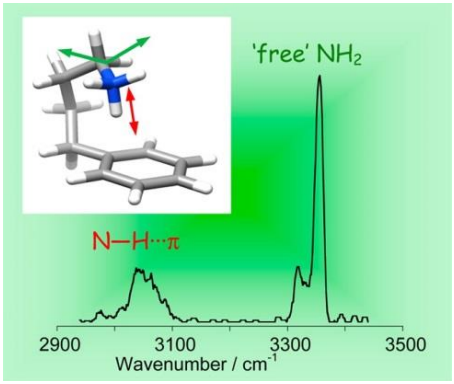

Figure 7. IRMPD spectrum and the most stable isomer of $C_6H_5(CH_2)_4NH_3^+$ calculated at the B3LYP/6-311++G(d,p) level of theory. Reprinted with permission from ref.26. Copyright 2014 American Chemical Society.

Studying hydrogen bonding is important because these interactions can be decisive for the conformational preferences and stability of biomolecules, including peptides.[27,28] Such a simple and defined gas-phase model as presented here may help in interpreting the IR spectra of more complex molecules and assessing the strength of these binding modes. For more examples, see below.

4. Metal complexes

Metal complexes play a key role in many synthetic and biological reactions because they are able to accept and release electrons. This ability can be further tuned by changing the coordination geometry of the ligands around the metal centre or by redox cooperation between metals and ligands. In this chapter, we will show that IRMPD spectroscopy can reveal the coordination modes of ligands.[29] We will also show that electron transfer between metals and ligands in complexes can be visualised in the corresponding IRMPD spectra. The spectra can be thus used to investigate redox processes crucial for biological models and for synthetic reactions.

4.1. Coordination geometry

Metals are the central part of metalloenzymes and one of the prominent bio-metals is zinc. Zinc prefers the oxidation state +II and, in contrast to other transition bio-metals, zinc is not redox-active. Zinc metalloenzymes are often active in bond-making and bond-breaking reactions (for example, dehydrogenases or aminopeptidases). Zinc acts as a Lewis acid and as a coordination centre. The coordination sphere around zinc usually has tetrahedral or trigonal bipyramidal geometry. The coordination sphere is mostly built from the side-chains of proline, aspartate, glutamate, and cysteine. Here, we will present a study of a zinc complex with imidazole ligands (Imi) and acetate (AcO^-). The model ligands were used to mimic the proline and aspartate/glutamate coordination sites.

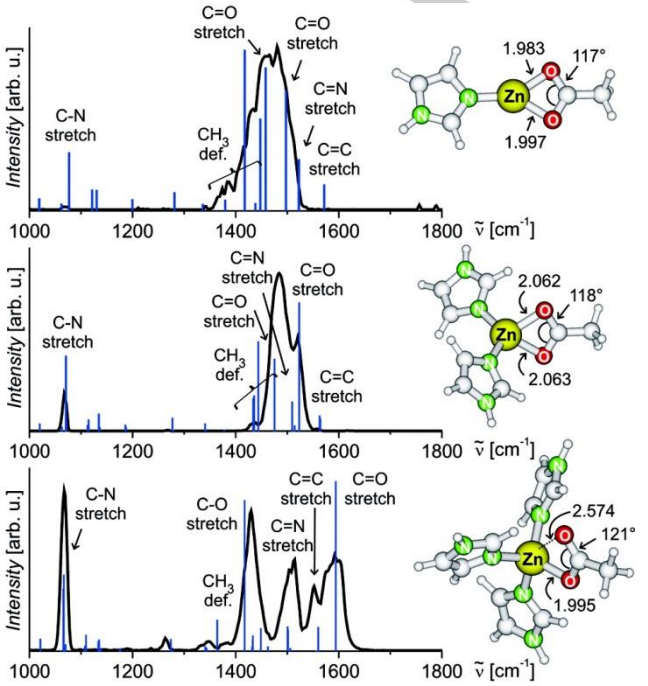

Figure 8. Experimental IRMPD spectra and theoretical IR spectra of (a) $[(Imi)Zn(CH_3COO)]^+$, (b) $[(Imi)_2Zn(CH_3COO)]^+$, and (c) $[(Imi)_3Zn(CH_3COO)]^+$. The structures show the computed minima for the corresponding ions with selected bond lengths expressed as Ångströms. Reprinted with permission from ref. 30. Copyright 2011 American Chemical Society.

Acetates, generally carboxylates, can coordinate as either bidentate or monodentate ligands. This dichotomy can be clearly observed in the IRMPD spectra of zinc complexes with acetate and with imidazole ligands $[(Imi)_nZn(AcO)]^+$ (Figure 8).[30] In the complex with one or two imidazole ligands, acetate coordinates to the zinc ions symmetrically and occupies two coordination sites. The symmetrical coordination is reflected in the respective IRMPD spectra as one broad band of the carboxylate vibration at approximately 1480 cm^{-1}. Adding a third imidazole ligand changes the coordination of acetate. Accordingly, we observe the stretching vibration of the C=O double bond (~1600 cm^{-1}) and the C-O single bond (~1430 cm^{-1}) in the IRMPD spectrum of $[(Imi)_3Zn(AcO)]^+$. This flexible coordination mode of acetate is termed carboxylate shift, which is important for many metal-carboxylate mediated reactions.[31]

One of the prominent metal-carboxylate-mediated reactions is C-H activation catalysed by palladium acetates or palladium trifluoroacetates. Most of these transformations were developed for systems with a remote coordination site to steer C-H activation selectivity. 2-Phenylpyridine (2-PhPy) is an example of such a system. Palladium acetate coordinates to the nitrogen atom of 2-phenylpyridine (Figure 9b).[32] The acetate ligand deprotonates the ortho-carbon atom of the phenyl ring via a six-membered transition structure (Figure 9c). The carboxylate shift is the essential reaction step because the bidentate-to-monodentate coordination change releases the carbonyl group

for the deprotonation reaction. Simultaneously, the vacated coordination site at the palladium atom assists the deprotonation reaction. The product of this reaction is a phenylpalladium complex with a neutral acetic acid ligand (Figure 9d).

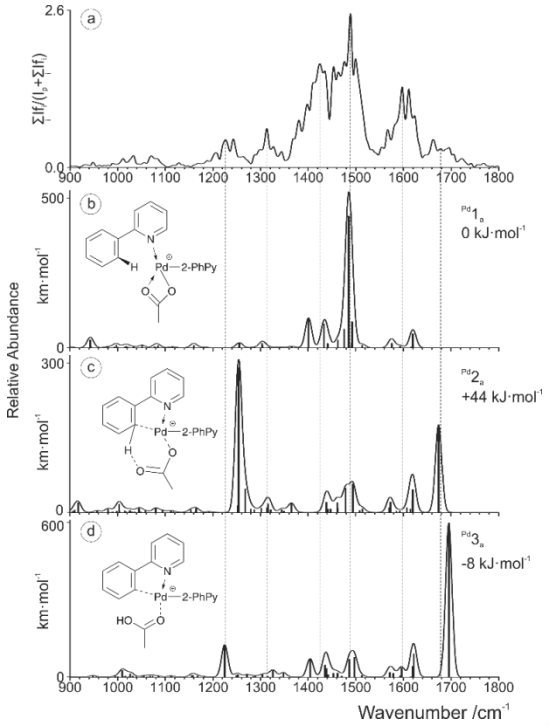

Figure 9. a) IRMPD spectrum of the mass-selected $[(2\text{-PhPy})_2Pd(OAc)]^+$ complex and b)-d) theoretical IR spectra of indicated palladium complexes. The line spectra are presented with a Gaussian function with fwhm = 16 cm^{-1}. Reprinted from ref. 32 published by The Royal Society of Chemistry.

The IRMPD spectrum of the model complex $[(2\text{-PhPy})2Pd(OAc)]^+$ shows signatures of both bidentate and monodentate coordination of acetate.[32] Thus, the spectrum shows a mixture of ions with intact 2-phenylpyridine ligands and ions with one C-H activated molecule of 2-phenylpyridine. This C-H activation was also studied in ruthenium acetate and copper acetate complexes. However, the IRMPD spectra of ruthenium and copper complexes only showed bidentate coordination of the acetate ligand and intact 2-phenylpyridine molecules.

The holy grail of C-H activation research is methane activation. Armentrout et al. investigated the activation of methane molecules by atomic platinum cation.[33] They demonstrated by IRMPD spectroscopy and theoretical calculations that the reaction of $Pt^+ + CH_4$ leads to dehydrogenation and to the formation of the platinum carbene cation, $PtCH_2^+$. Adding a second methane molecule to $PtCH_2^+$ also leads to C-H bond activation. During this process, one hydrogen atom migrates from the incoming methane molecule to the carbene group, thereby forming the $Pt(CH_3)_2^+$ cation. A third methane molecule does not react with platinum. Instead, it only adds to the platinum atom, thus forming the $Pt(CH_3)_2(CH_4)^+$ complex. The structure of this complex can be clearly identified from the IRMPD spectrum of the mass-selected platinum complex (Figure10).

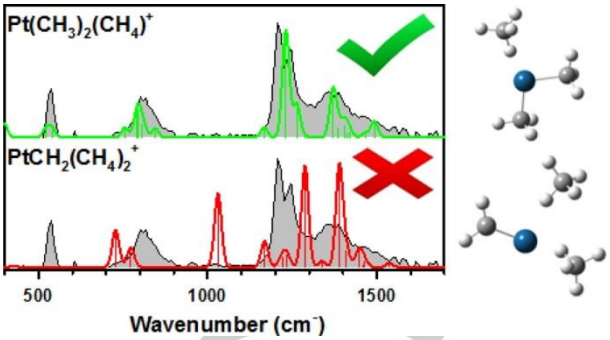

Figure 10. IRMPD spectrum for $[Pt,3C,10H]^+$ (in shade) and theoretical IR spectra of the low-lying isomer (in green and red) calculated at the B3LYP/def2-TZVPPD level of theory. Reprinted with permission from ref.33. Copyright 2016 American Chemical Society.

4.2. Metal complexes with redox active ligands

One of the prototypical redox active biometals is copper. Copper metalloenzymes are involved in several processes, including photosynthesis and respiration. In the oxidation reactions, copper cooperates with ligands, for example in galactose oxidase, in which the interplay between copper and the phenoxy radical, derived from tyrosine side-chain, plays a key role.[34,35] Copper may have either +I or +II oxidation states in biosystems. In each oxidation state, copper has different coordination sphere; linear or tetrahedral for +I state and tetragonal/octahedral for +II state. Changes in the coordination sphere may induce changes in the oxidation state and vice versa.

A small, three-component system $[Cu(PhO)(L)]^+$ (L = ligand) exemplifies the effect of the coordination geometry around copper on its redox reactivity. $[Cu(PhO)(L)]^+$ complexes with a monodentate ligand L (for example, water or pyridine) have linear coordination geometry at the copper centre. This coordination favours the oxidation state +I; therefore, the phenoxy ligand has a radical character. The IRMPD spectra of $[Cu(PhO)(H_2O)]^+$ and $[Cu(PhO)(Py)]^+$ show a strong band of the phenoxy C-O vibration at approximately 1500 cm^{-1}, which is the frequency typical for the phenoxy radical (Figure11).[35] The bidentate ligand *N*,*N*,*N*′,*N*′-tetramethylethylenediamine (TMEDA) has been used to change the coordination geometry. The trigonal coordination of the $[Cu(PhO)(TMEDA)]^+$ complex no longer favours the +I oxidation state of copper. Instead, copper is in the +II oxidation state and the phenoxy ligand is reduced to the phenolate anion. This redox reaction can be observed in the IRMPD spectrum of $[Cu(PhO)(TMEDA)]^+$. The phenoxy C-O stretching is located at 1270 cm^{-1}. Hence, the C-O frequency is redshifted by more than 200 cm^{-1} with respect to the linearly coordinated copper(I) complexes. These results show that the C-O stretching vibration can be used as a spectral marker for the redox state in copper-phenoxy type complexes.

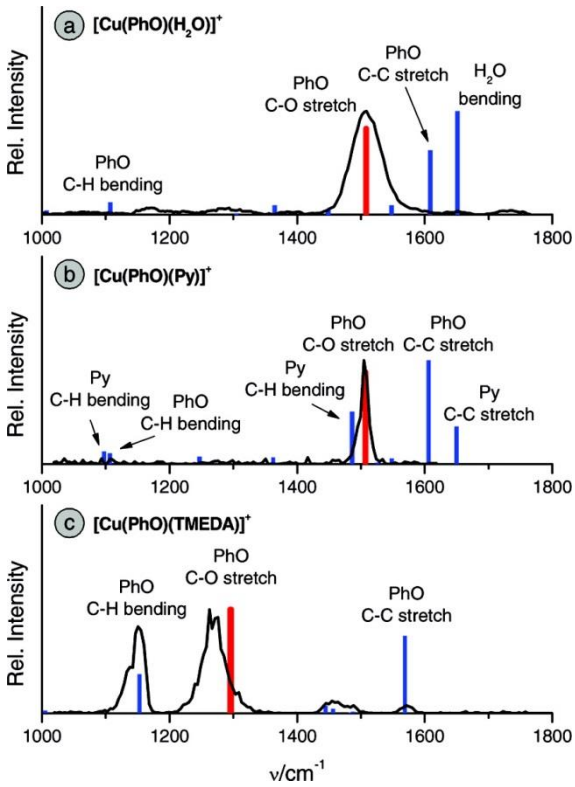

Figure 11. IRMPD and computed IR spectra of $[Cu(PhO)(H_2O)]^+$ (a), $[Cu(PhO)(Py)]^+$ (b), and $[Cu(PhO)(TMEDA)]^+$ (c). Reprinted with permission from ref.35. Copyright 2008 American Chemical Society.

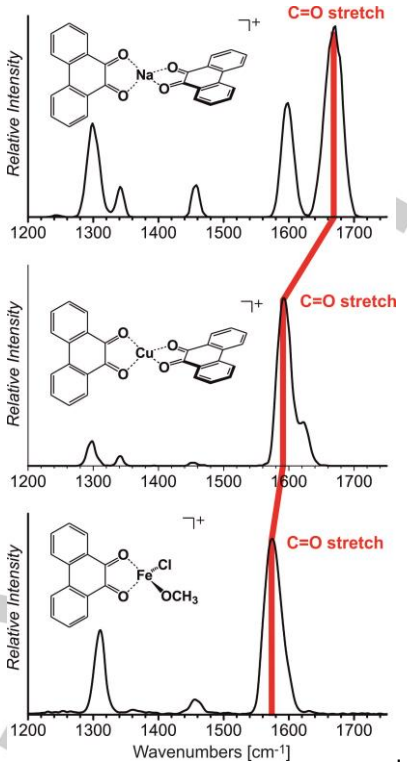

Figure 12. IRMPD spectra of sodium, copper(I), and iron(III) complexes with phenanthraquinone. The red bar indicates the carbonyl stretching bands of the complexes. Adapted with permission from refs. 36 and 37. Copyright 2009 American Chemical Society and Copyright 2016 Elsevier.

Another class of ligands capable of redox activity with metals are quinones. Quinones can accept two electrons stepwise, sequentially forming semiquinones and diol-diates. This behaviour was studied for ortho-quinone phenanthraquinone (PQ) in complexes with sodium, copper and iron (Figure 12).[36,37] Sodium cation can only be in the +I oxidation state. Accordingly, the binding in the $[(PQ)_2Na]^+$ complex is dominated by ion-dipole interactions. The C=O stretching band of $[(PQ)_2Na]^+$ is found at 1670 cm^{-1}. Copper(I) in the analogous complex $[(PQ)_2Cu]^+$ is redox active and can be oxidised. Copper oxidation requires PQ reduction to the semiquinone form. This reaction would be associated with a decrease in the bond order of the carbonyl bonds. We can observe that this interaction partly contributes to the binding in $[(PQ)_2Cu]^+$ because the stretching vibration of the C=O bond redshifts to 1600 cm^{-1}.

A red shift of the carbonyl stretching vibration to 1580 cm^{-1} can also be observed in the spectrum of the iron complex $[(PQ)Fe(CH_3O)(Cl)]^+$ (Figure 12). It was shown that this complex dissociates in the gas phase by formaldehyde and HCl elimination, thereby yielding the $[(PQ)Fe]^+$ complex. This process is enabled by the redox activity of iron-phenanthraquinone couple, and the resulting complex $[(PQ)Fe]^+$ consists of iron(II) and the semiquinone radical anion $PQ^{\bullet-}$.[37]

4.3. Metal complexes as intermediates in organometallic reactions

Intermediates in organometallic reactions are another important example from the field of metal complexes. In this section, we show the application of IRMPD spectroscopy to the study of gold-catalysed reactions. Homogeneous gold catalysis became a key tool in nucleophilic additions to alkynes and related reactions. Nucleophilic additions coupled with the introduction of an oxygen atom were also developed. These reactions are initiated by adding an oxidation reagent such as pyridine *N*-oxide to gold(I)-activated alkynes (Scheme 3). These oxidation reagents consist of oxygen and a leaving group (here: pyridine). The elimination of the leaving group leads to gold(I) α-oxo carbene intermediates. These intermediates can either undergo hydrogen rearrangement to form α,β-unsaturated ketones or couple with a nucleophile to form α-substituted ketones (Scheme 3).[38]

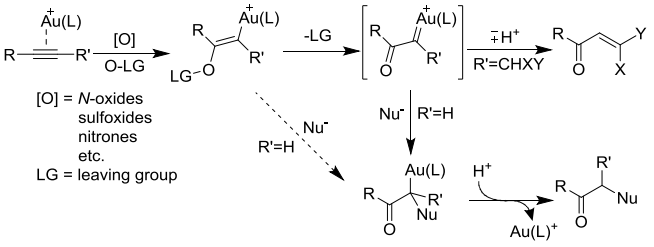

Scheme 3. Gold(I) catalysed oxidation of alkynes via gold(I) α-oxo carbenes intermediates. Adapted with permission from refs. 38. Copyright 2014 American Chemical Society.

Gold(I) α-oxo carbene intermediates have never been experimentally detected in condensed phase because of their high reactivity. Conversely, ions with a *m/z* ratio corresponding to the gold(I) α-oxo carbene intermediates can be easily detected by ESI-MS in the gas phase. The structure of these ions was investigated by IRMPD spectroscopy, and the results showed that no gold(I) α-oxo carbene intermediates could be trapped because they immediately rearranged to more stable ions.

Figure 13 shows an example of putative gold(I) α-oxo carbene intermediates. These complexes were formed from their precursors $[(IPr)Au(alkyne)(PyO)]^+$ (IPr: see Figure 13 for the ligand structure; alkyne = 1-phenylpropyne or 2-butyne) by collision-induced dissociation (CID) in the gas phase. The IRMPD spectra clearly show that the attempt to trap gold(I) α-oxo carbene complexes with a phenyl group next to the carbene atom had failed. Such complex rearranges to a more stable ketene complex (see Figure 13a-c). If the carbon atom next to the carbene atom bears a hydrogen atom, then, even more facile rearrangements become possible. The hydrogen atom rearranges to the carbene atom, and we observe the formation of α,β-unsaturated ketones (Figure 13d-f). Hence, the IRMPD spectra show that gold(I) α-oxo carbenes cannot be isolated in the gas phase. Subsequent studies showed that the intermediates could not be isolated in the condensed phase either because they immediately couple with the leaving group of the oxidation reagent (for example pyridine from pyridine *N*-oxide) or with a solvent molecule.[39]

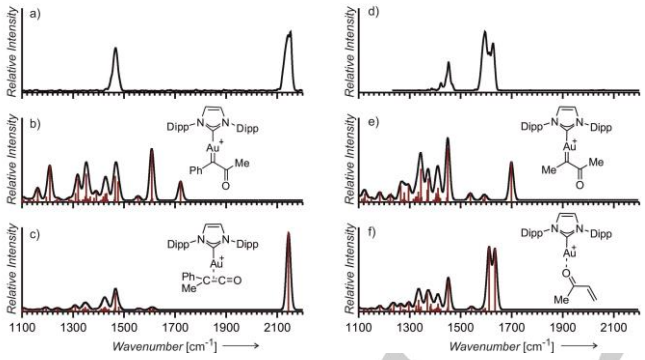

Figure 13. a) IRMPD spectrum of $[(IPr)Au(PhCCMe,O)]^+$ (m/z 717) generated by CID from $[(IPr)Au(PhCCMe,PyO)]^+$; b) and c) predicted IR spectra of relevant ion structures in the gas phase; d) IRMPD spectrum of $[(IPr)Au(MeCCMe,O)]^+$ (m/z 655) generated by CID from $[(IPr)Au(MeCCMe,PyO)]^+$; e) and f) predicted IR spectra of relevant ion structures in the gas phase. Adapted with permission from refs. 38. Copyright 2014 American Chemical Society.

5. Towards bio-applications

Classical mass spectrometry, instrumentation and methods, is shifting towards structural biology. Accordingly, most newly developed methods have targeted applications for biomolecules. This is also true for IRMPD spectroscopy. The advantages of IRMPD spectroscopy were shown in studies on (de)protonation and metal-binding sites of biologically relevant molecules and in studies on local intramolecular interactions in amino acids and peptides,[40] in nucleobases and nucleotides,[41] and in neurotransmitters.[42] IRMPD spectroscopy was also used to study biological intermediates of the nitrosation of amino acids, peptides or cofactors such as heme.[43] In this chapter, we will focus on recent examples of using IRMPD spectroscopy with free electron lasers to best understand the structure of biologically relevant molecules.

5.1. Small molecules in complex mixtures – towards metabolomics

Mass spectrometry is a powerful method frequently used in metabolomics, particularly when seeking to identify the signature of key chemical compounds associated with diseases in blood samples.[44] Mass spectrometry is also applied to assess the metabolism of drugs in biological samples. Metabolite identification can be challenging because they often have low concentrations (in the μM – nM range). Mass spectrometry can detect these compounds and determine their fragmentation patterns. However, this is insufficient for unknown compounds. In contrast, NMR spectroscopy can identify compounds unequivocally, yet it is less sensitive than mass spectrometry and usually requires micrograms of the isolated compound. Thus, combining mass spectrometry with IRMPD spectroscopy can be an effective alternative that preserves the sensitivity of mass spectrometry and additionally provides IR spectra. Such combination may suffice to identify unknown compounds.

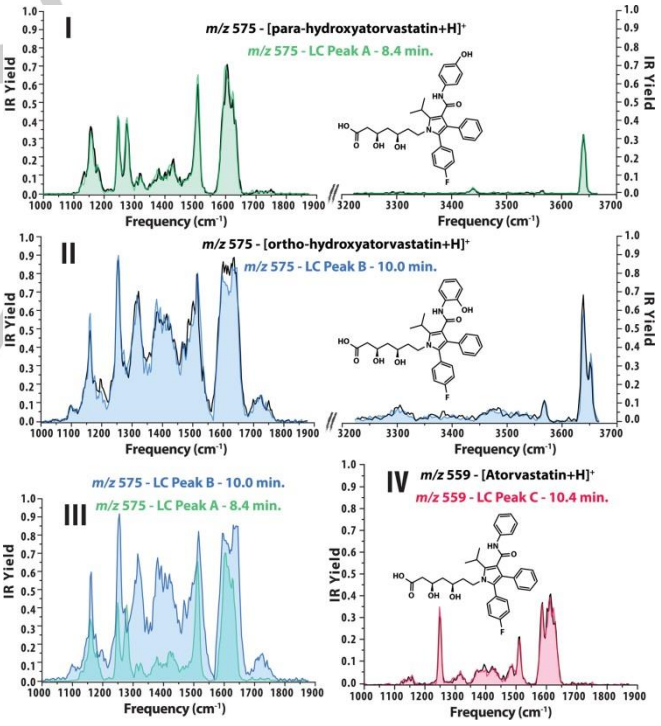

Figure 14. Panels I and II present IR spectra (coloured traces) generated for ions at *m/z* 575 from two fractions of LC, and the isobaric drug metabolites identified based on IR spectral match reference compounds (black traces). Panel III highlights the difference in IR spectra of the two isomeric metabolites. Panel IV contains the IR spectrum measured for unmetabolised atorvastatin. Reprinted with permission from ref. 45. Copyright 2017 American Chemical Society.

This approach was recently applied to identify the metabolites of atorvastatin, an inhibitor used as a lipid-lowering

drug.[45] Atorvastatin is metabolised by hydroxylation at cytochrome P450 3A4 to *ortho*- and *para*-hydroxylated molecules. The authors were able to separate these two hydroxylated metabolites by liquid chromatography (LC) and identify their structure by IRMPD spectroscopy (Figure 14). They showed that the *ortho*- and *para*-hydroxylated metabolites have different IR spectra and that the spectra can be readily distinguished in the fingerprint and in the higher frequency range of the IRMPD spectra (Figure 14). They also showed that the MS/MS approach provides no clue to the identification of these different isomers. The identification using the LC-IRMPD approach required nanograms of metabolites, which is beyond the reach of the alternative LC-NMR method. This study shows that the LC-IRMPD approach is a promising alternative for the "identification of small molecules buried in complex mixtures".[45]

5.2. Metal complexes of bio-relevant molecules

Cisplatin (*cis*-$[Pt(NH_3)Cl_2]$) is likely the most known anticancer drug. This drug was discovered 40 years ago, and it is still used nowadays. Cisplatin is partly hydrolysed when entering a cell forming biologically active *cis*-$[Pt(NH_3)(H_2O)Cl]^+$. This complex was characterised by IRMPD spectroscopy.[46] Cisplatin interacts with DNA at the N7 position of adenine (A) and guanine (G). However, the exact structures of the complexes between cisplatin and the nucleobases are not known. Electrospray ionisation of a solution of cisplatin with adenine or guanine provides complexes *cis*-$[Pt(NH_3)_2(A)Cl]^+$ and *cis*-$[Pt(NH_3)_2(G)Cl]^+$, thereby IRMPD spectroscopy could have been used to identify how cisplatin interacts with the nucleobases.[47]

Chiavarino et al. confirmed that platinum interacts with the N7 position of guanine in *cis*-$[Pt(NH_3)_2(G)Cl]^+$ (Figure 15). In addition, they observed a red shift of the carbonyl stretch of guanine and of the N-H stretch of the NH_3 ligand of the platinum complex. This red-shift is consistent with the hydrogen binding between the ammonia ligand and the carbonyl oxygen. In contrast, the adenine complex, *cis*-$[Pt(NH_3)_2(A)Cl]^+$, does not profit from such hydrogen-bonding stabilisation. Instead, two isomeric structures were identified with platinum coordinated either to the N3 or to the N1 position of adenine.

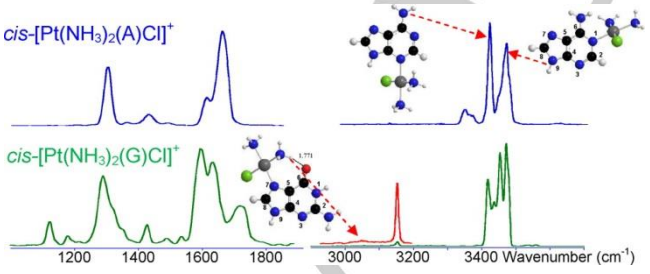

Figure 15. Experimental IRMPD spectra of *cis*-$[Pt(NH_3)_2(A)Cl]^+$ (in blue) and *cis*-$[Pt(NH_3)_2(G)Cl]^+$ (in green and red); the low-lying isomers were calculated at the B3LYP/6-311G** level of theory. Reprinted with permission from ref. 47. Copyright 2013 American Chemical Society.

On the way from the simple platinum-nucleobase complexes towards platinum-nucleotide complexes, the number of coordinating groups in the complexes increases.[48] The reaction between 2′-deoxyguanosine-5′-monophosphate (5′-dGMP) and cisplatin yields two types of complexes; *cis*-$[Pt(NH_3)_2(5'\text{-dGMP-H})]^+$ and *cis*-$[PtCl(NH_3)_2(5'\text{-dGMP})]^+$. In both complexes, platinum coordinates to the N7 position of guanine, as determined for the simple *cis*-$[Pt(NH_3)_2(G)Cl]^+$ complex (see above). However, the phosphate groups also play a key stabilisation role. In the *cis*-$[Pt(NH_3)_2(5'\text{-dGMP-H})]^+$ complex, the phosphate anion directly coordinates to platinum. The arrangement of the ammonia ligands enables strong hydrogen bonding between one of the ammonia ligands and the carbonyl function of guanine (as observed for *cis*-$[Pt(NH_3)_2(G)Cl]^+$). In the second complex, *cis*-$[PtCl(NH_3)_2(5'\text{-dGMP})]^+$, the phosphate does not coordinate to platinum directly, but instead forms hydrogen bonds with the ammonia ligands. Accordingly, the hydrogen bonding between the ammonia ligands and the carbonyl function of guanine is much weaker than in the former complex, which is clearly evidenced by the relative positions of the carbonyl stretching bands in the IRMPD spectra (Figure 16). Similar structural studies were also conducted for complexes with other biologically relevant molecules, such as aminoacids and oligonucleotides.[49]

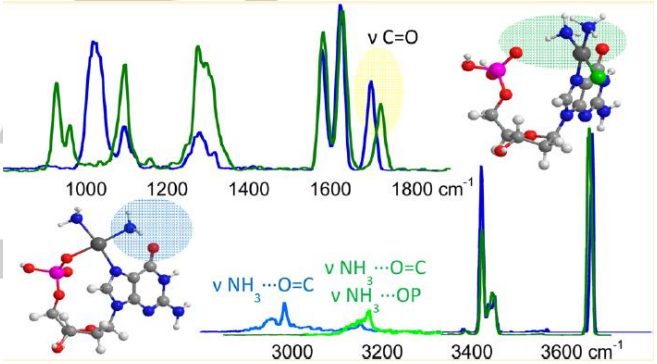

Figure 16. IRMPD spectra of *cis*-$[Pt(NH_3)_2(5'\text{-dGMP-H})]^+$ (blue lines) and *cis*-$[PtCl(NH_3)_2(5'\text{-dGMP})]^+$ (green lines). Reprinted with permission from ref 48. Copyright 2015 American Chemical Society.

5.3. Towards biomolecules

Mass spectrometry analysis of large molecules has recently benefited from the implementation of ion mobility. Ion mobility allows us to determine the overall size and shape of molecules. However, the method provides no information on specific interactions affecting the secondary structure of biomolecules. In this context, IRMPD spectroscopy can be complementary to ion mobility and complete the overall picture of the structure of a biomolecule.

Protein structure and dynamics are determined by various attractive and repulsive interactions within the molecular backbone. IRMPD spectroscopy is useful to detect the characteristic protein bands *amide I* (usually at approximately 1650 cm^{-1}; C=O stretching) and *amide II* (usually at approximately 1550 cm^{-1}; N-H bending). These bands serve as spectral markers of the helical structure of proteins.[50,51,52]

IRMPD spectroscopy was used to determine the secondary structure of multiply protonated ubiquitin and cytochrome c (Figure 17).[52] The IRPMD spectra of both biomolecules at low and intermediate charge states (denoted by L and I in Figure 17) show the typical *amide I* and *II* bands. However, in the intermediate state, another *amide II* band appears. This band, denoted as *IIa*, is red-shifted (~1480 cm^{-1}) with respect to the original *amide II* band (denoted as *IIb*). This

red-shifted band prevails at high charge states (H) of the biomolecules. The authors showed that the amide *IIa* bands originate from extended (not helical) sub-structures of the proteins. Hence, the IRMPD spectra show how the protonated proteins lose their helical structure with the increase in the charge of their backbones.

The described charge-induced unzipping of proteins is a gas-phase phenomenon and, therefore, could be considered irrelevant, at first sight. However, protein structure is often investigated and determined by mass spectrometry. Proteins are often transferred to the gas phase at high charge states; therefore, accounting for the unzipping is crucial for the evaluation of protein structures.

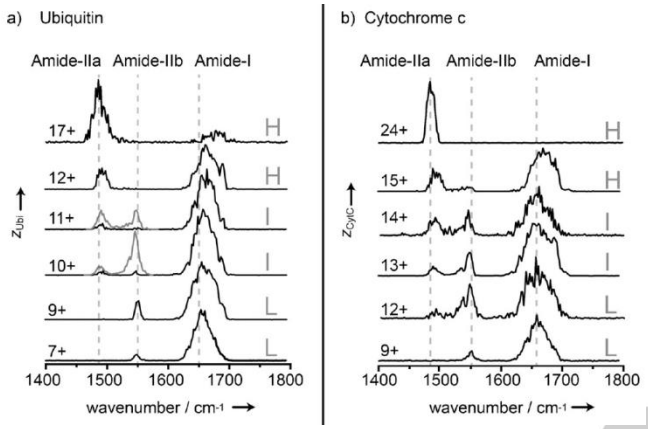

Figure 17. IR spectra of a) ubiquitin and b) cytochrome c for various charge states. Gray trace segments for ubiquitin 10+ and 11+ denote a higher photon density. Three types of bands identified are labelled *amide IIa*, *amide IIb*, and *amide I*. Reprinted from ref. 52.

IRMPD spectroscopy was also applied to examine the gas-phase structure of G-quadruplex. G-quadruplex is a structural motif of DNA with characteristic G-quartets formed by four guanine bases bound together by hydrogen bonds.[53] This structural motif occurs in guanine-rich nucleic acid sequences such as the human telomeric sequence dTTAGGGTTAGGGTTAGGGTTAGGG (denoted as T_4). Gabelica at el. studied the effect of electrospray ionisation and gas-phase conditions on the structure of T_4.[54] The authors were able to obtain gaseous $[T_4(NH_4^+)_2]^{5-}$ and $[T_4]^{5-}$. Both anions were generated from aqueous ammonium acetate solutions of T_4; $[T_4(NH_4^+)_2]^{5-}$ is formed at soft ionisation conditions and $[T_4]^{5-}$ at hard ionisation conditions. The IRMPD spectra of these two anions are different, and the main differences were detected in the range of carbonyl vibrations (Figure 18).

In order to evaluate the carbonyl spectral signatures, the authors compared the results to the IRMPD spectrum of single strand T_1 in which no hydrogen-bonded guanine sub-structures could be formed. This spectrum shows two carbonyl stretching bands (1710 cm^{-1}: thymine_1) and (1735 cm^{-1}: thymine_2 + guanine). Non-interacting guanine bases are characterised by a band at 1735 cm^{-1}. This band decreases in relative intensity in the IRMPD spectrum of $[T_4]^{5-}$. The change in band intensities was explained by a red-shift of guanine carbonyl stretching vibrations due to hydrogen bonding. The IRMPD spectrum of $[T_4(NH_4^+)_2]^{5-}$ shows an even larger red shift of the carbonyl stretches (to 1685 cm^{-1}). The comparison between the spectra shows that this large red shift is characteristic of guanine quartets, whereas the smaller red shift in $[T_4]^{5-}$ reflects only partial preservation of the hydrogen bonding network. Hence, this study shows that the ammonium ions are essential for preserving the G-quadruplex structure of DNA.[55]

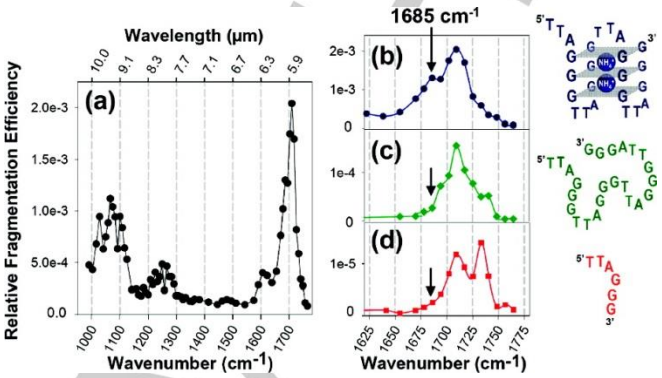

Figure 18.. IRMPD spectra of telomeric DNA sequences. a) Full spectrum of $[(T_4)(NH_4^+)_2]^{5-}$. b-d) Zooms on the carbonyl stretch regions of b) $[T_4(NH_4^+)_2]^{5-}$, c) $[T_4]^{5-}$, and d) $[T_1]^{2-}$. Reprinted with permission from ref. 54. Copyright 2008 American Chemical Society.

6. Towards solution

Lastly, we show how IRMPD spectroscopy can contribute to answering a key question in mass spectrometry research. The question is how relevant are the results obtained in the gas-phase, if we are actually interested in the properties of molecules/ions naturally occurring in the condensed phase? How relevant is the structure of an ion solved by IRMPD spectroscopy? The approach to assess the effect of solvation on the structure of an ion is to investigate complexes of this ion with a gradually increasing number of solvent molecules. IRMPD spectroscopy is an ideal tool to assess this “microsolvation” effect because, as shown in all sections above, it can easily unravel changes in protonation sides and coordination or binding modes.[56] The studies discussed below exemplify analyses of microsolvation effects that led to significant changes in ion structures. Only few publications have reported insignificant changes upon microsolvation;[57,58] however, this primarily results from the low attractiveness rather than the scarcity of these results. Furthermore, it should be noted that extensive spectroscopical studies have been conducted for various charged water clusters.[59] Those studies did not use free-electron lasers and, therefore, are outside the scope of this review.

6.1. Microsolvation effect

Returning to the first topic of this review, the following questions must be answered: where is the charge? how relevant are the detected ions with respect to the ions present in solution? Chang et al. elegantly demonstrated the effect of solvent molecules on the structure of the protonated methyl ester of *p*-aminobenzoic acid (as well as other aromatic amines).[60] The molecule is protonated at the nitrogen atom in solution (Scheme 4). Isolated molecules in the gas phase are

protonated at the ester group due to the stabilisation of the positive charge by electron delocalisation (Scheme 4).

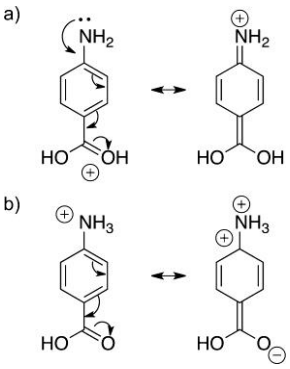

Scheme 4. Resonance contributors for $PABAH^+$ protonated at (a) the carboxylic acid or at (b) the amine. Reprinted with permission from ref. 60. Copyright 2012 American Chemical Society.

Chang et al. showed that the change of the protonation mode in solution is caused by stabilisation of protonation at the amino group by hydrogen bonding with solvent molecules.[60] It takes three molecules of water to stabilise N-protonated form (Figure 19; note that these results were obtained with OPO photon source, not with FEL). The charge at the ammonium group is stabilised by hydrogen bonding between ammonium hydrogen atoms and solvent molecules. Hydrogen bonding with less than three molecules of water (*i.e.* some hydrogen atom(s) of the ammonium group does not have a partner for hydrogen bonding) is not sufficient to override the stabilisation of the gas-phase structure by electron delocalisation.

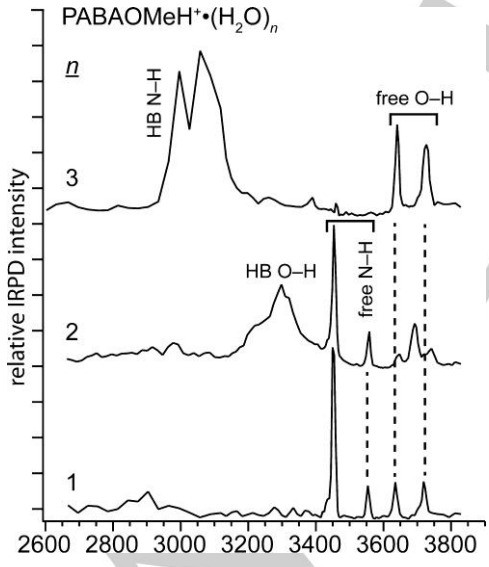

Figure 19. Infrared photodissociation spectra of $PABAOMeH^+.(H_2O)_{1\text{-}3}$ at 133 K. Reprinted with permission from ref. 60. Copyright 2012 American Chemical Society.

The number of required water molecules is not determined by the ammonium group only. The structure of the remaining part of the molecules plays a key role. A small change, such as hydrolysis of the ester to *p*-aminobenzoic acid, leads to dramatic changes. Protonation of the carboxyl group is the preferred mode in the gas phase. This form prevails upon microsolvation with up to five molecules of water. Only the sixth molecule of water inverts the stabilities, and *N*-protonated molecules start to prevail in the gas phase, as observed in solution. This results from the acidic hydrogen at the carboxylic group that requires stabilisation by hydrogen bonding in the gas phase also. If we extrapolate this evidence on the structural stability of molecules from solution to the gas phase to the context of biomolecules, we conclude that many molecules will likely be required for a reliable snapshot from solution rather than gas phase-specific structures.[57]

Another interesting issue refers to ions in the atmosphere, wherein microsolvation (or better microhydration) plays a key role. These ions are in the gas phase, but their reactivity is considerably affected by interactions with water molecules and water droplets. IRMPD spectroscopy helps us understand their spectroscopic characteristics. For example, Heine et al. showed how the symmetrical proton-bound nitrate dimer ($[NO_3^-\text{-}H^+\text{-}NO_3^-]$) changes, by interaction with additional HNO_3 or H_2O molecules, into the nitrate anion stabilised by interactions with neutral molecules (Figure 20).[61]

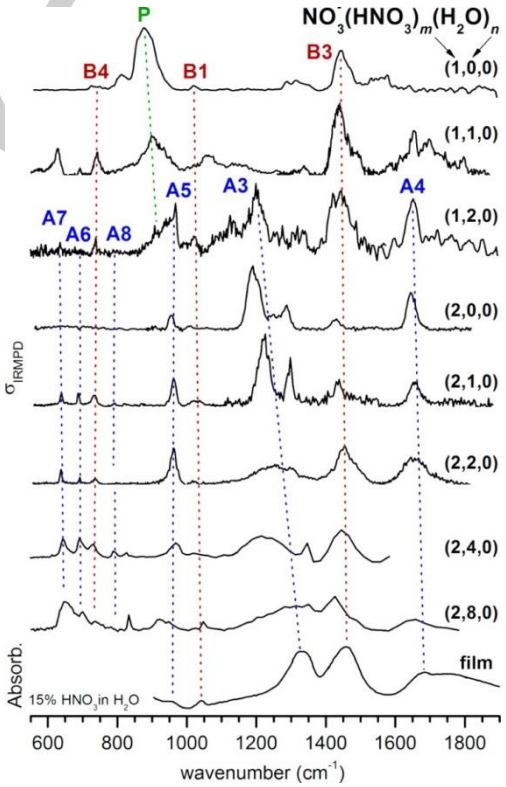

Figure 20. Experimental IRMPD spectra of $NO_3^-(HNO_3)_m(H_2O)_n$ clusters m = 1,2, n = 1-8 (top panels) compared to absorption spectra of amorphous 15% HNO_3 in H_2O. Peaks are labelled according to their assignment to modes of the neutral acid molecule (**A**) or of the conjugate base anion (**B**), or to the shared proton stretching mode (**P**). Reprinted with permission from ref. 61. Copyright 2014 American Chemical Society.

The IRMPD spectra of the $[(NO_3)(HNO_3)_m(H_2O)_n]^-$ clusters show that proton sharing between two nitrate anions is preferred only if the complex is naked (*i.e.* m=1, n=0) or when it is

solvated by just one molecule of H_2O (*i.e.* *m*=1, *n*=1). The proton bound dimer displays itself by the shared-proton stretching mode located at approximately 900 cm^{-1} (green P in Figure 20). Interaction with more molecules of either HNO_3 or H_2O leads to the stabilisation of the cluster with one nitrate anion, whilst the other molecules remain neutral. Neutral nitric acid has several characteristic bands (blue A letters in the spectra in Figure 20) that appear only after adding two water molecules. Simultaneously, the band of the shared proton disappears. Increasing the number of water molecules in the cluster leads to an IRMPD spectrum that resembles the IR spectrum in the condensed phase (see the bottom spectra in Figure 20). Similar findings were also reported for the microsolvation of the proton-bound sulfate dimer.[62]

8. Prospects of IRMPD spectroscopy with free electron lasers

The introduction of free-electron lasers in ion spectroscopy has markedly increased the use of IRMPD spectroscopy. While broadening applications of IRMPD spectroscopy have been developed, its weak points have also been increasingly identified, which, in our opinion, are (1) the multiphotonic character[63] and (2) the low resolution of the method. Both these weaknesses can be overcome by using tagging methods and laboratory light sources, such as optical parametric oscillators (OPOs) and meanwhile many laboratories use this approach to record IR spectra of ions.[64] The challenge for IRMPD spectroscopy at free-electron laser facilities is, therefore, to find and explore research fields that are not accessible in laboratory setups.

One of the exclusive characteristics of FELs is the availability of photons at the low-frequency range (wavenumber below 600 cm^{-1}). The measurements of IRMPD spectra in this range provide opportunities to detect stretching vibrations of bonds involving heavy metals or even metal-metal bonds. This might be important for research on metal clusters and reactivity involving metal clusters.[65]

Measurements using IRMPD spectra with FELs are fast. The scan over the entire fingerprint range takes approximately 20 minutes (the exact time may vary with the signal intensity). Such rapid scanning is advantageous for experiments with small amounts of available sample (for example, in the detection of metabolites, as shown in section 5.1.).

IRMPD spectroscopy experiments with FELs require no special mass-spectrometry setup. The experiments are usually conducted in standard quadrupole ion traps or in ion cyclotron resonance (ICR) mass spectrometers. Thus, IRMPD spectra can be measured for all ions that can be detected by this type of instruments without additional experimental requirements. This versatility (and also availability) was at the origin of the boom in research on small molecules by IRMPD-spectroscopy. Now and in future, the same reasons may lead to a boom in research on biomolecules by IRMPD-spectroscopy.

Acknowledgements ((optional))

The authors thank the European Research Council (ERC CoG No. 682275) for support of their work, Rafael Navrátil for the frontispiece graphics and Dr. Carlos V. Melo for proofreading the manuscript.

Keywords: biomolecules • gas phase • IRMPD spectroscopy • metal complexes • solvation

10.1002/chem.201705692

WILEY-VCH

Entry for the Table of Contents

MINIREVIEW

Infrared multiphoton dissociation spectroscopy has evolved from a tool used to study the structure of small ions to a method that enables us to assess biomolecules. Here, we review the development of IRMPD and show examples of studies along this path, from simple problems to applications in metabolomics and atmospheric chemistry.

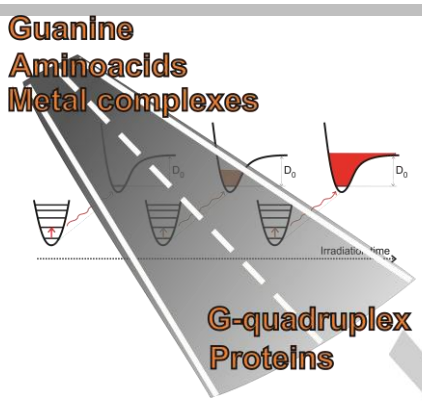

*Lucie Jašíková, Jana Roithová**

Page No. – Page No.

Infrared multiphoton dissociation spectroscopy with free electron lasers: On the road from small molecules to biomolecules

References

[1] D. W. Lupo, M. Quack, *Chem. Rev.* **1987**, *87*, 181-216.

[2] a) H. A. Schwarz, *J. Chem. Phys.* **1977**, *67*, 5525-5534; b) T. Oka, *Phys. Rev. Lett.* **1980**, *45*, 531-534; c) M. Okumura, L. I. Yeh, Y. T. Lee, *J. Chem. Phys.* **1985**, *83*, 3705-3706; d) L. I. Yeh, J. M. Price, Y. T. Lee, *J. Am. Chem. Soc.* **1989**, *111*, 5597-5604.

[3] a) J. Oomens, D. T. Moore, G. Meijer, G. von Helden, *Phys. Chem. Chem. Phys.* **2004**, *6*, 710-718; b) B. Lucas, G. Grégoire, J. Lemaire, P. Maitre, J. M. Ortega, A. Rupenyan, B. Reimann, J. P. Schermann, C. Desfrançois, *Phys. Chem. Chem. Phys.* **2004**, *6*, 2659-2663.

[4] E. J. Bieske, J. P. Maier, *Chem. Rev.* **1993**, *93*, 2603-2621;

[5] M. A. Duncan, *J. Phys. Chem. A* **2012**, *116*, 11477-11491;

[6] a) M. Katari, E. Nicol, V. Steinmetz, G. van der Rest, D. Carmichael, G. Frison, *Chem. Eur. J.* **2017**, *23*, 8414-8423; b) A. Sharma, G. Ohanessian, C. Clavaguera, *J. Mol. Model.* **2014**, *20*, 2426-2435; c) F. Aguilar-Galindo, M. M. Montero-Campillo, M. Yáñez, O. Mó, *Chem. Phys. Lett.* **2014**, *598*, 91-95; d) A. Cimas, P. Maitre, G. Ohanessian, M. P. Gaigeot, *J. Chem. Theory Comput.* **2009**, *5*, 2388-2400.

[7] a) R. K. Sinha, D. Scuderi, P. Maitre, B. Chiavarino, M. E. Crestoni, S. Fornarini, *J. Phys. Chem. Lett.* **2015**, *6*, 1605-1610; b) D. Morsa, V. Gabelica, F. Rosu, J. Oomens, E. De Pauw, *J. Phys. Chem. Lett.* **2014**, *5*, 3787-3791; c) M. J. van Stipdonk, M. J. Kullman, G. Berden, J. Oomens, *Rapid Commun. Mass Spectrom.* **2014**, *28*, 691-698; d) C. A. Austin, Y. Chen, C. M. Kaczan, G. Berden, J. Oomens, M. T. Rodgers, *Int. J. Mass Spectrom.* **2013**, *354-355*, 346-355; e) M. E. Crestoni, B. Chiavarino, J. Lemaire, P. Maitre, S. Fornarini, *Chem. Phys.* **2012**, *398*, 118-123; f) B. E. Ziegler, R. A. Marta, S. M. Martens, J. K. Martens, T. B. McMahon, *Int. J. Mass Spectrom.* **2012**, *316-318*, 117-125; g) H. Yao, J. D. Steill, J. Oomens, R. A. Jockusch, *J. Phys. Chem. A* **2011**, *115*, 9739-9747; h) M. Seydou, G. Grégoire, J. Liquier, J. Lemaire, J. P. Schermann, C. . Desfrançois, *J. Am. Chem. Soc.* **2008**, *130*, 4187-4195; i) M. Seydou, J. C. Gillet, X. Li, H. Wang, G. H. Posner, G. Grégoire, J. P. Schermann, K. H. Bowen, C. Desfrançois, *Chem. Phys. Lett.* **2007**, *449*, 286-290.

[8] D. Schröder, M. Buděšínský, J. Roithová, *J. Am. Chem. Soc.* **2012**, *134*, 15897-15905.

[9] Z. Tian, S. R. Kass, *J. Am. Chem. Soc.* **2008**, *130*, 10842-10843.

[10] J. D. Steill, J. Oomens, *J. Am. Chem. Soc.* **2009**, *131*, 13570-13571.

[11] J. Oomens, G. Berden, T. H. Morton, *ChemPhysChem* **2015**, *16*, 1992-1995.

[12] J. Oomens, G. Berden G., T. H. Morton, *Angew. Chem. Int. Ed.* **2017**, *56*, 217-220.

[13] a) R. A. Marta, R. Wu, K. R. Eldridge, J. K. Martens, T. B. McMahon, *Phys. Chem. Chem. Phys.* **2010**, *12*, 3431-3442; b) T. D. Fridgen, T. B. McMahon, L. MacAleese, J. Lemaire, P. Maitre, *J. Phys. Chem. A* **2004**, *108*, 9008-9010.

[14] Review: a) N. C. Polfer, *Chem. Soc. Rev.* **2011**, *40*, 2211-2221; b) K. Gulyuz, C. N. Stedwell, D. Wang, N. C. Polfer, *Rev. Sci. Instrum.* **2011**, *82*, 054101-054107; c) N. C. Polfer, J. Oomens, *Mass Spectrom. Rev.* **2009**, *28*, 468-494; d) R. Wu, T. B. McMahon, *Mass Spectrom. Rev.* **2009**, *28*, 546-585; e) T. D. Fridgen, *Mass Spectrom. Rev.* **2009**, *28*, 586-607; f) J. R. Eyler, *Mass Spectrom. Rev.* **2009**, *28*, 448-467.

[15] For some recent papers see: a) A. F. DeBlase, C. P. Harribal, J. T. Lawler, N. L. Burke, S. A. McLuckey, T. S. Zwier, *J. Am. Chem. Soc.* **2017**, *139*, 5481-5493; b) K. J. D. Fouque, H. Lavanant, S. Zirah, V. Steinmetz, S. Rebuffat, P. Maitre, C. Afonso, *J. Phys. Chem. A* **2016**, *120*, 3810-3816; c) W. Fu, J. Xiong, M. J. Lecours, P. J. J. Carr, R. A. Marta, E. Fillion, T. McMahon, V. Steinmetz, W. S. Hopkins, *J. Mol. Spectrosc.* **2016**, *330*, 194-199; d) R. Feng, H. Yin, X. Kong, *Rapid Commun. Mass Spectrom.* **2016**, *30*, 24-28; e) H. Yin, Z. Kong, *J. Am. Soc. Mass Spectrom.* **2015**, *26*, 1455-1461; f) A. Masson, M. Z. Kamrath, M. A. S. Perez, M. S. Glower, U. Rothlisberger, D. E. Clemmer, T. R. Rizzo, *J. Am. Soc. Mass Spectrom.* **2015**, *26*, 1444-1454; g) E. Kleisath, R. A. Marta, S. Martens, J. Martens, T. McMahon, *J. Phys. Chem.* A **2015**, *119*, 6689-6702; h) W. S. Hopkins, R. A. Marta, T. B. McMahon, *J. Phys. Chem. A* **2013**, *117*, 10714-10718; i) B. Yang, R. R. Wu, G. Berden, J. Oomens, M. T. Rodgers, *J. Phys. Chem. B* **2013**, 117, 14191-14201.

[16] T. R. Rizzo, J. A. Stearns, O. V. Boyarkin, *Int. Rev. Phys. Chem.* **2009**, *28*, 481-515.

[17] P. Hurtado, F. Gámez, S. Hamad, B. Martínez-Haya, J. D. Steill., J. Oomens, *J. Phys. Chem. A* **2011**, *115*, 7275-7282.

[18] S. M. Craig, F. S. Menges, C. H. Duong, J. K. Denton, L. R. Madison, A. B. McCoy, M. A. Johnson, *Proc. Natl. Acad. Sci. U. S. A.* **2017**, *114*, E4706-E4713.

[19] a) C. T. Wolke, J. A. Fournier, L. C. Dzugan, M. R. Fagiani, T. T. Odbadrakh, H. Knorke, K. D. Jordan, A. B. McCoy, K. R. Asmis, M. A. Johnson, *Science* **2016**, *354*, 1131-1135; b) R. Shishido, Y. Kawai, A. Fujii, *J. Phys. Chem. A* **2014**, *118*, 7297-7305.

[20] S. G. Olesen, T. L. Guasco, J. R. Roscioli, M. A. Johnson, *Chem. Phys. Lett.* **2011**, *509*, 89-95.

[21] D. A. Wild, K. T. Kuwata, C. K. Wong, J. D. Lobo, A. Deev, T. S. Schindler, M. Okumura, E. J. Bieske, *J. Phys. Chem. A* **2010**, *114*, 4762-4769.

[22] M. Demireva, J. Oomens, G. Berden, E. R. Williams, *ChemPlusChem* **2013**, *78*, 995-1004.

[23] For example: B. Chiavarino, M. E. Crestoni, S. Fornarini, J. Lemaire, L. Mac Aleese,
P. Maitre, *ChemPhysChem* **2005**, *6*, 437-440.

[24] B. Chiavarino, M. E. Crestoni, S. Fornarini, J. Lemaire, P. Maitre, L. MacAleese, *J. Am. Chem. Soc.* **2006**, *128*, 12553-12561.

[25] a) M. Burt, K. Wilson, R. Marta, M. Hasan, W. Scott Hopkins, T. McMahon, *Phys. Chem. Chem. Phys.* **2014**, *16*, 24223-24234; b) B. Chiavarino, M. E. Crestoni, P. Maître, S. Fornarini, *Int. J. Mass Spectrom.* **2013**, *354-355*, 62-69.

[26] B. Chiavarino, M. E. Crestoni, M. Schütz, A. Bouchet, S. Piccirillo, V. Steinmetz, O. Dopfer, S. Fornarini, *J Phys Chem A* **2014**, *118*, 7130-7138.

[27] S. Jaeqx, W. Du, E. J. Meijer, J. Oomens, A. M. Rijs, *J. Phys. Chem. A* **2013**, *117*, 1216-1227.

[28] W. Fu, P. J. J. Carr, M. J. Lecours, M. Burt, R. A. Marta, V. Steinmetz, E. Fillion, T. B. McMahon, W. S. Hopkins, *Phys. Chem. Chem. Phys.* **2017**, *19*, 729-734.

[29] a) L. Jašíková, E. Hanikýřová, A. Škríba, J. Jašík, J. Roithová, *J. Org. Chem.* **2012**, *77*, 2829-2836; b) A. J. Ross, F. Dreiocker, M. Schäfer, J. Oomens, A. J. H. M. Meijer, B. T. Pickup, R. F. W. Jackson, *J. Org. Chem.* **2011**, *76*, 1727-1734; c) A. R. Massah, F. Dreiocker, R. F. W. Jackson, B. T. Pickup, J. Oomens, A. J. H. M. Meijer, M. Schäfer, *Phys. Chem. Chem. Phys.* **2011**, *13*, 13255-13267; d) A. Lagutschenkov, U. J. Lorenz, O. Dopfer, *Int. J. Mass Spectrom.* **2011**, *308*, 316-329; e) L. Ducháčková, J. Roithová, P. Milko, J. Žabka, N. Tsierkezos, D. Schröder, *Inorg. Chem.* **2011**, *50*, 771-782; f) T. E. Cooper, D. R. Carl, J. Oomens, J. D. Steill, P. B. Armentrout, *J. Phys. Chem. A* **2011**, *115*, 5408-5422; g) F. Dreiocker, J. Oomens, A. J. H. M. Meijer, B. T. Pickup, R. F. W. Jackson, M. Schäfer, *J. Org. Chem.* **2010**, *75*, 1203-1213; h) L. Ducháčková, V. Steinmetz, J. Lemaire, J. Roithová, *Inorg. Chem.* **2010**, *49*, 8897-8903.

[30] L. Ducháčková, D. Schröder, J. Roithová, *Inorg. Chem.* **2011**, *50*, 3153-3158.

[31] J. Paterová, J. Heyda, P. Jungwirth, C. J. Schaffer, Á. Révész, E. L. Zins, D. Schröder, *J. Phys. Chem. A* **2011**, *115*, 6813-6819.

[32] A. Gray, A. Tsybizová, J. Roithová, *Chem. Sci.* **2015**, *6*, 5544-5553.

[33] O. W. Wheeler, M. Salem, A. Gao, J. M. Bakker, P. B. Armentrout, *J. Phys. Chem. A* **2016**, *120*, 6216-6227.

[34] P. Milko, J. Roithová, D. Schröder, J. Lemaire, H. Schwarz, M. C. Holthausen, *Chem. Eur. J.* **2008**, *14*, 4318-4327.

[35] P. Milko, J. Roithová, N. Tsierkezos, D. Schröder, *J. Am. Chem. Soc.* **2008**, *130*, 7186-7187.

[36] G. Yassaghi, L. Jašíková, J. Roithová, *Int. J. Mass. Spectrom.* **2016**, *407*, 92-100.

[37] P. Milko, J. Roithová, *Inorg. Chem.* **2009**, *48*, 11734-11742.

[38] J. Schulz, L. Jašíková, A. Škríba, J. Roithová, *J. Am. Chem. Soc.* **2014**, *136*, 11513–11523.

[39] J. Schulz, J. Jašík, A. Gray, J. Roithová, *Chem. Eur. J.* **2016**, *22*, 9827–9834.

[40] For some recent papers see: a) G. C. Boles, C. J. Owen, G. Berden, J. Oomens, P. B. Armentrout, *Phys. Chem. Chem. Phys.* **2017**, *19*, 12394-12406; b) A. Bouchet, J. Klyne, S. Ishiuchi, M. Fujii, O. Dopfer, *Phys. Chem. Chem. Phys.* **2017**, *19*, 10767-10776; c) W. Fu, P. J. J. Carr, M. J. Lecours, M. Burt, R. A.

Marta, V. Steinmetz, E. Fillion, T. B. McMahon, W. S. Hopkins, *Phys. Chem. Chem. Phys.* **2017**, *19*, 729-734; d) M. Lesslie, J. T. Lawler, A. Dang, J. A. Korn, D. Bím, V. Steinmetz, P. Maitre, F. Tureček, *ChemPhysChem* **2017**, *18*, 1293-1301; e) P. G. Wenthold, D. Koirala, A. Somogyi, J. C. Poutsma, *J. Phys. Org. Chem.* **2017**, *30*, 3606-3611; f) B. Gregori, L. Guidoni, M. E. Crestoni, P. de Oliveira, C. Houée-Levin, D. Scuderi, *J. Phys. Chem. B* **2017**, *121*, 2083-2094; g) H. Li, J. Jiang, Y. Luo, *Phys. Chem. Chem. Phys.* **2017**, *19*, 15030-15038; h) J. C. Poutsma, J. Martens, J. Oomens, P. Maitre, V. Steinmetz, M. Bernier, M. Jia, V. Wysocki, *J. Am. Soc. Mass Spectrom.* **2017**, *28*, 1482-1488; i) K. Peckelsen, J. Martens, G. Berden, J. Oomens, R. C. Dunbar, A. J. H. M. Meijer, M. Schäfer, *J. Mol. Spectrosc.* **2017**, *332*, 38-44; j) G. C. Boles, R. A. Coates, G. Berden, J. Oomens, P. B. Armentrout, *J. Phys. Chem. B* **2016**, *120*, 12486-12500; k) A. P. Cismesia, L. S. Bailey, M. R. Bell, L. F. Tesler, N. C. Polfer, *J. Am. Soc. Mass Spectrom.* **2016**, *27*, 757-766; l) M. C. Bernier, J. Chamot-Rooke, V. H. Wysocki, *Phys. Chem. Chem. Phys.* **2016**, *18*, 2202-2209; m) L. J. M. Kempkes, J. K. Martens, J. Grzetic, G. Berden, J. Oomens, *Rapid Commun. Mass Spectrom.* **2016**, *30*, 483-490; n) M. Lesslie, J. K. C. Lau, J. T. Lawler, K. W. M. Siu, V. Steinmetz, P. Maitre, A. C. Hopkinson, V. Ryzhov, *ChemPlusChem* **2016**, *81*, 444-452; o) D. Scuderi, J. Bergés, P. de Oliveira, C. Houée-Levin, *Radiat. Phys. Chem.* **2016**, *128*, 103-111; p) C. J. Shaffer, J. Martens, A. Marek, J. Oomens, F. Tureček, *J. Am. Chem. Soc. Mass Spectrom.* **2016**, *27*, 1176-1185; q) R. A. Coates, G. C. Boles, C. P. McNary, G. Berden, J. Oomens, P. B. Armentrout, *Phys. Chem. Chem. Phys.* **2016**, *18*, 22434-22445; r) J. Gao, G. Berden, M. T. Rodgers, J. Oomens, *Phys. Chem. Chem. Phys.* **2016**, *18*, 7269-7277; s) Y. Jami-Alahmadi, B. D. Linford, T. D. Fridgen, *J. Phys. Chem. B* **2016**, *120*, 13039-13046; t) R. C. Dunbar, J. Martens, G. Berden, J. Oomens, *Phys. Chem. Chem. Phys.* **2016**, *18*, 26923-26932; u) Y. Jami-Alahmadi, T. D. Fridgen, *Phys. Chem. Chem. Phys.* 2016, 18, 2023-2033; v) G. C. Boles, R. A. Coates, G. Berden, J. Oomens, P. B. Armentrout, *J. Phys. Chem. B* **2015**, *119*, 11607-11617; w) R. C. Dunbar, *Int. J. Mass Spectrom.* **2015**, *377*, 159-171; x) M. B. Burt, T. D. Fridgen, *Eur. J. Mass Spectrom.* **2012**, *18*, 235-250.

[41] For some recent papers see: a) B. Power, S. Rowe, T. D. Fridgen, *J. Phys. Chem. B* **2017**, *121*, 58-65; b) Y. Zhu, L. A. Hamlow, C. C. He, J. K. Lee, J. Gao, G. Berden, J. Oomens, M. T. Rodgers, *J. Phys. Chem. B* **2017**, *121*, 4048-4060; c) A. Ciavardini, A. D. Cort, S. Fornarini, D. Scuderi, A. Giardini, G. Forte, E. Bodo, S. Piccirillo, *J. Mol. Spectrosc.* **2016**, *120*, 8892-8904; d) Y. Zhu, L. A. Hamlow, C. C. He, S. F. Strobehn, J. K. Lee, J. Gao, G. Berden, J. Oomens, M. T. Rodgers, *J. Phys. Chem. B* **2016**, *121*, 4048-4060; e) R. R. Wu, C. C. He, L. A. Hamlow, Y.-w. Nei, G. Berden, J. Oomens, M. T. Rodgers, *Phys. Chem. Chem. Phys.* **2016**, *18*, 15081-15090; f) R. R. Wu, C. C. He, L. A. Hamlow, Y.-w. Nei, G. Berden, J. Oomens, M. T. Rodgers, *J. Phys. Chem. B* **2016**, *120*, 4616-4624; g) R. R. Wu, M. T. Rodgers, *J. Phys. Chem. B* **2016**, *120*, 4803-4811; h) R. R. Wu, B. Yang, C. E. Frieler, G. Berden, J. Oomens, M. T. Rodgers, *J. Am. Chem. Soc. Mass Spectrom.* **2016**, *27*, 410-421; i) B. Power, V. Haldys, J.-Y. Salpin, T. D. Fridgen, *J. Mass Spectrom.* **2016**, *51*, 236-244; j) Y. Nosenko, C. Riehn, G. Niedner-Schatteburg, *Phys. Chem. Chem. Phys.* **2016**, *18*, 8491-8501; k) C. M. Kaczan, A. I. Rathur, R. R. Wu, Y. Chen, C. A. Austin, G. Berden, J. Oomens, M. T. Rodgers, *Int. J. Mass Spectrom.* **2015**, *378*, 76-85; l) M. Berdakin, V. Steinmetz, P. Maitre, G. A. Pino, *Phys. Chem. Chem. Phys.* **2015**, *17*, 25915-25924; m) M. R. Ligare, A. M. Rijs, G. Berden, M. Kabeláč, D. Nachtigallová, J. Oomens, M. S. de Vries, *J. Phys. Chem. B* **2015**, *119*, 7894-7901; n) B. Power, V. Haldys, J.-Y. Salpin, T. D. Fridgen, *Int. J. Mass Spectrom.* **2015**, *378*, 328-335; o) J. Y. Salpin, D. Scuderi, *Rapid Commun. Mass Spectrom.* **2015**, *29*, 1898-1904; p) H. U. Ung, K. T. Huynh, J. C. Poutsma, J. Oomens, G. Berden, T. H. Morton, *Int. J. Mass Spectrom.* **2015**, *378*, 294-302; q) R. R. Wu, B. Yang, G. Berden, J. Oomens, M. T. Rodgers, *J. Phys. Chem. B* **2015**, *119*, 2795-2805; r) R. R. Wu, B. Yang, C. E. Frieler, G. Berden, J. Oomens, M. T. Rodgers, *Phys. Chem. Chem. Phys.* **2015**, *17*, 25978-25988; s) B. E. Ziegler, R. A. Marta, M. B. Burt, S. M. Martens, J. K. Martens, T. B. McMahon, *J. Am. Soc. Mass Spectrom.* **2014**, *25*, 176-185; t) M. Berdakin, V. Steinmetz, P. Maitre, G. A. Pino, *J. Phys. Chem. A* **2014**, *118*, 3804-3809; u) J. Y. Salpin, V. Haldys, S. Guillaumont, J. Tortajada, M. Hurtado, A. M. Lamsabhi, *ChemPhysChem* **2014**, *15*, 2959-2971; v) J. Y. Salpin, L. MacAleese, F. Chirot, P. Dugourd, *Phys. Chem. Chem. Phys.* **2014**, *16*, 14127-14138; w) R.R. Wu, B. Yang, G. Berden, J. Oomens, M. T. Rodgers, *J. Phys. Chem. B* **2014**, *118*, 14774-14784; x) Y. Nosenko, F. Menges, C. Riehn, G. Nieder-Schatteburg, *Phys. Chem. Chem. Phys.* **2013**, *15*, 8171-8178; y) A. Filippi, C. Fraschetti, F. Rondino, S. Piccirillo, V. Steinmetz, L. Guidoni, M. Speranza, *Int. J. Mass Spectrom.* **2013**, *354-355*, 54-61; z) F. Lanucara, M. E. Crestoni, B. Chiavarino, S. Fornarini, O. Hernandez, D. Scuderi, P. Maitre, *RSC Adv.* **2013**, *3*, 12711-12720; aa) Y.-w. Nei, K. T. Crampton, G. Berden, J. Oomens, M. T. Rodgers, *J. Phys. Chem. A* **2013**, *117*, 10634-10649; ab) H. U. Ung, A. R. Moehlig, R. A. Kudla, L. J. Mueller, J. Oomens, G. Berden, T. H. Morton, *Phys. Chem. Chem. Phys.* **2013**, *15*, 19001-19012; ac*)* O. Y. Ali, T. D. Fridgen, *ChemPlusChem* **2012**, *13*, 588-596.

[42] a) M. Schütz, A. Bouchet, B. Chiavarino, M. E. Crestoni, S. Fornarini, O. Dopfer, *Chem. Eur. J.* **2016**, *22*, 8124-8136; b) A. Lagutschenkov, J. Langer, G. Berden, J. Oomens, O. Dopfer, *Phys. Chem. Chem. Phys.* **2011**, *13*, 2815-2823; c) A. Lagutschenkov, J. Langer, G. Berden, J. Oomens, O. Dopfer, *Phys. Chem. Chem. Phys.* **2011**, *13*, 15644-15656; d) A. Lagutschenkov, J. Langer, G. Berden, J. Oomens, O. Dopfer, *J. Phys. Chem. A* **2010**, *114*, 13268-13276.

[43] a) M. E. Crestoni, B. Chiavarino, S. Fornarini, *Pure Appl. Chem.* **2015**, *87*, 379-390; b) B. Gregorim, L. Guidoni, B. Chiavarino, D. Scuderi, E. Nicol, G. Frison, S. Fornarini, M. E. Crestoni, *J. Phys. Chem. B* **2014**, *118*, 12371-12382; c) B. Chiavarino, M. E. Crestoni, S. Fornarini, *Croat. Chem. Acta* **2014**, *87*, 307-314; d) F. Lanucara, D. Scuderi, B. Chiavarino, S. Fornarini, P. Maitre, M. E. Crestoni, *J. Phys. Chem. Lett.* **2013**, *4*, 2414-2417; e) F. Lanucara, B. Chiavarino, M. E. Crestoni, D. Scuderi, R. K. Sinha, P. Maitre, S. Fornarini, *Int. J. Mass Spectrom.* **2012**, 330-332, 160-167.

[44] For some recent papers see: a) H. C. Liao, Z. Spacil, F. Ghomashchi, M. L. Escolar, J. Kurtzberg, J. J. Orsini, F. Tureček, C. R. Scott, M. H Gelb, *Clin. Chem.* **2017**, *63*, 1363-1369; b) Y. Liu, F. Yi, A. B. Kumar, N. K. Chennamaneni, X. Y. Hong, C. R. Scott, M. H. Gelb, F. Tureček, *Clin. Chem.* **2017**, *63*, 1118-1126; c) S. Elliott, N. Buroker, J. J. Cournoyer, A. M. Potier, J. D. Trometer, C. Elbin, M. J. Schermer, J. Kantola, A. Boyce, F. Tureček, M. H. Gelb, C. R. Scott, *Mol. Genet. Metab.* **2016**, *118*, 304-309; d) Z. Spacil, A. B. Kumar, H. C. Liao, C. Auray-Blais, S. Stark, T. R. Suhr, C. R. Scott, F. Tureček, M. H. Gelb, *Clin. Chem.* **2016**, *62*, 279-286; e) M. H. Gelb, C. R. Scott, F. Tureček, *Clin. Chem.* **2015**, *61*, 335-346.

[45] J. Martens, V. Koppen, G. Berden, F. Cuyckens, J. Oomens, *Anal. Chem.* **2017**, *89*, 4359-4362.

[46] a) D. Corinti, C. Coletti, N. Re, S. Piccirillo, M. Giampá, M. E. Crestoni, S. Fornarini, *RSC Adv.* **2017**, *7*, 15877-15884; b) D. Corinti, C. Coletti, N. Re, B. Chiavarino, M. E. Crestoni, S. Fornarini, *Chem. Eur. J.* **2016**, *22*, 3794-3803; c) A. De Petris, A. Ciavardini, C. Coletti, N. Re, B. Chiavarino, M. E. Crestoni, S. Fornarini, *J. Phys. Chem. Lett.* **2013**, *4*, 3631-3635.

[47] B. Chiavarino, M. E. Crestoni, S. Fornarini, D. Scuderi, J. Y. Salpin, *J. Am. Chem. Soc.* **2013**, *135*, 1445-1455.

[48] B. Chiavarino, M. E. Crestoni, S. Fornarini, D. Scuderi, J. Y. Salpin, *Inorg. Chem.* **2015**, *54*, 3513-3522.

[49] a) D. Corinti, A. De Petris, C. Coletti, N. Re, B. Chiavarino, M. E. Crestoni, S. Fornarini, *ChemPhysChem* **2017**, *18*, 318-325; b) A. E. Egger, C. G. Hartinger, H. B. Hamidane, Y. O. Tsybin, B. K. Keppler, P. J. Dyson, *Inorg. Chem.* **2008**, *47*, 10626-10633.

[50] J. Seo, W. Hoffmann, S. Warnke, M. T. Bowers, K. Pagel, G. von Helden, *Angew. Chem. Int. Ed.* **2016**, *55*, 14173-14176.

[51] S. Warnke, W. Hoffmann, J. Seo, E. De Genst, G. von Helden, K. Pagel, *J. Am. Soc. Mass Spectrom.* **2017**, *28*, 638-646.

[52] A. I. González Flórez, E. Mucha, D. S. Ahn, S. Gewinner, W. Schöllkopf, K. Pagel, G. von Helden, *Angew. Chem. Int. Ed.* **2016**, *55*, 3295-3299.

[53] M. Rueda, F. J. Luque, M. Orozco, *J. Am. Chem. Soc.* **2006**, *128*, 3608-3619.

[54] V. Gabelica, F. Rosu, E. De Pauw, J. Lemaire, J. C. Gillet, J. C. Poully, F. Lecomte, G. Grégoire, J. P. Schermann, C. Desfrançois, *J. Am. Chem. Soc.* **2008**, *130*, 1810-1811.

[55] V. Gabelica, E. S. Baker, M. P. Teulade-Fichou, E. De Pauw, M. T. Bowers, *J. Am. Chem. Soc.* **2007**, *129*, 895-904.

[56] a) S. T. Sun, L. Jiang, J. W. Liu, N. Heine, T. I. Yacovitch, T. Wende, K. R. Asmis, D. M. Neumark, Z. F. Liu, *Phys. Chem. Chem. Phys.* **2015**, *17*, 25714-25724; b) D. Schröder, L. Ducháčková, J. Tarábek, M. Karwowska, K. J. Fijalkowski, M. Ončák, P. Slavíček, *J. Am. Chem. Soc.* **2011**, *133*, 2444-2451; c) C. J. Shaffer, D. Schröder, *Int. J. Mass Spectrom.* **2012**, *311*, 17-23; d) G. S. Groenewold, M. J. Van Stipdonk, W. A. de Jong, J. Oomens, G. L. Gresham,

M. E. McIlwain, D. Gao, B. Siboulet, L. Visscher, M. Kullman, N. Polfer, *ChemPhysChem* **2008**, *9*, 1278-1285; e) T. D. Fridgen, T. B. McMahon, P. Maitre, J. Lemaire, *Phys. Chem. Chem. Phys.* **2006**, *8*, 2483-2490.

[57] M. B. Moghaddam, T. D. Fridgen, *J. Phys. Chem. B* **2013**, *117*, 6157-6164.

[58] M. Butler, P. A. Mañez, G. M. Cabrera, P. Maitre, *J. Phys. Chem. A* **2014**, *118*, 4942-4954.

[59] For example: a) J. W. Shin, N. I. Hammer, E. G. Diken, M. A. Johnson, R. S. Walters, T. D. Jaeger, M. A. Duncan, R. A. Christie, K. D. Jordan, *Science* **2004**, *304*, 1137-1140; b) J. M. Headrick, E. G. Diken, R. S. Walters, N. I. Hammer, R. A. Christie, J. Cui, E. M. Myshakin, M. A. Duncan, M. A. Johnson, K. D. Jordan, *Science* **2005**, *308*, 1765-1769;

[60] T. M. Chang, J. S. Prell, E. R. Warrick, E. R. Williams, *J. Am. Chem. Soc.* **2012**, *134*, 15805-15813.

[61] N. Heine, T. I. Yacovitch, F. Schubert, C. Brieger, D. M. Neumark, K. R. Asmis, *J. Phys. Chem. A* **2014**, *118*, 7613-7622.

[62] T. I. Yacovitch, N. Heine, C. Brieger, T. Wende, C. Hock, D. M. Neumark, K. R. Asmis, *J. Phys. Chem. A* **2013**, *117*, 7081-7090.

[63] C. J. Shaffer, Á. Révész, D. Schröder, L. Severa, F. Teplý, E. L. Zins, L. Jašíková, J. Roithová, *Angew. Chem. Int. Ed.* **2012**, *51*, 10050-10053.

[64] For selected examples, see a) E. Andris, R. Navrátil, J. Jašík, G. Sabenya, M. Costas, M. Srnec, J. Roithová, *Angew. Chem. Int. Ed.* **2017**, *56*, 14057-14060; b) E. Andris, R. Navrátil, J. Jašík, T. Terencio, M. Srnec, M. Costas, J. Roithová, *J. Am. Chem. Soc.* **2017**, *139*, 2757-2765; c) J. Klyne, O. Dopfer, *J. Mol. Spectrosc.* **2017**, *337*, 124-136 ; d) R. J. Cooper, J. T. O´Brien, T. M. Chang, E. R. Williams, *Chem. Sci.* **2017**, *8*, 5201-5213; e) M. R. Fagiani, X. Song, P. Petkov, S. Debnath, S. Gewinner, W. Schöllkopf, T. Heine, A. Fielicke, K. R. Asmis, *Angew. Chem. Int. Ed.* **2017**, *56*, 501-504; f) S. Ye, C. Kupper, S. Meyer, E. Andris, R. Navrátil, O. Krahe, B. Mondal, M. Atanasov, E. Bill, J. Roithová, F. Meyer, F. Neese, *J. Am. Chem. Soc.* **2016**, *138*, 14312-14325.

[65] For selected examples, see: a) J. D. Harding, T. R. Walsh, S. M. Hamilton, W. S. Hopkins, S. R. Mackenzie, P. Gruene, M. Haertelt, G. Meijer, A. Fielicke, *J. Chem. Phys.* **2010**, *132*, 011101; b) P. Claes, E. Janssens, V. T. Ngan, P. Gruene, J. T. Lyon, D. J. Harding, A. Fielicke, M. T. Nguyen, P. Lievens, *Phys. Rev. Lett.* **2011**, *107*, 173401; c) Asmis K. R., *Phys. Chem. Chem. Phys.* **2012**, *14*, 9270-9281; d) L. M. Ghiringhelli, P. Gruene, J. T. Lyon, D. M. Rayner, G. Meijer, A. Fielicke, M. Scheffler, *New J. Phys.* **2013**, *15*, 083003; e) B. Helmich, M. Sierka, J. Döbler, J. Sauer, *Phys. Chem. Chem. Phys.* **2014**, *16*, 8441; f) bCalvo F., L. Yejun, D. M. Kiawi, J. M. Bakker, P. Parneix, E. Janssens, *Phys. Chem. Chem. Phys.* **2015**, *17*, 25956-25967; g) W. S. Hopkins, P. J. J. Carr, D. Huang, K. P. Bishop, M. Burt, T. B. McMahon, V. Steinmetz, E. Fillion, *J. Phys. Chem. A* **2015**, *119*, 8469-8475; h) K. Koyma, T. Nagata, S. Kudoh, K. Miyajima, D. M. M. Huitema, V. Chernyy, J. M. Bakker, F. Mafuné, *J. Phys. Chem. A* **2016**, *120*, 8599-860.